

# Journal of Mechanics of Materials and Structures

**A REFINED 1D BEAM THEORY BUILT ON 3D SAINT-VENANT'S SOLUTION TO  
COMPUTE HOMOGENEOUS AND COMPOSITE BEAMS**

Rached El Fatmi

**Volume 11, No. 4**

**July 2016**



# A REFINED 1D BEAM THEORY BUILT ON 3D SAINT-VENANT'S SOLUTION TO COMPUTE HOMOGENEOUS AND COMPOSITE BEAMS

RACHED EL FATMI

This paper proposes a refined 1D beam theory (RBT) built on the 3D Saint-Venant (SV) solution established for arbitrary composite cross-section. In this theory (RBT/SV), the displacement model introduces sectional out-of-plane warpings, Poisson's effects and distortions. For a given cross-section, the sectional displacement modes are extracted from the computation of the correspondent 3D SV's solution. These sectional modes, which reflect the mechanical behavior of the cross-section, lead to a beam theory that really fits the section nature (shape and material(s)). As a result, RBT/SV allows to recover a more realistic spatial behavior for the beam, to catch a significant part of the edge effects, and hence to compute a relatively short beam. In order to apply RBT/SV, a package (named CSB) of two complementary numerical Matlab tools have been developed: CSection and CBeam. CSection computes by 2D-FEM the deformation modes of the cross-section, and CBeam uses these sectional modes to generate the correspondent beam theory and compute by 1D-FEM the beam. A significant set of homogeneous/composite beams have been computed and, to show the efficiency of such a theory, 3D RBT/SV results have been systematically compared with those provided by full 3D-FEM computations.

## 1. Introduction

Nowadays, the design of homogeneous beams is well understood and the calculation methods available for engineers are sufficient to meet the requirements of current mechanical engineering, even if walled profiles are not completely under control (especially when thin/thick and open/closed multicellular sections are involved).

In contrast, composite beams are not so easy to design. Their mechanical behavior is much more difficult to understand and to predict. Laminated composite beams are known to exhibit complex phenomena such as coupled deformations arising from the anisotropic nature of the layers and from the stacking sequences. And the situation is more complex when, to reduce cost and weight, thin-walled open/closed composite sections are involved. Detailed structural models are then essential in order to fully exploit such specific effects in the design phase. In addition to the structural level, detailed 3D stress analysis is of practical relevance for laminated composites and especially the interlaminar stresses which may result in delamination and failure of the laminates.

Today, using composite beams is a real trend in many engineering applications but the use of 3D finite element (3D-FEM) analysis to facilitate design is costly. This trend calls for the development of a realistic general beam theory and efficient numerical tools, suitable for the analysis of beams exhibiting 3D effects, for which the classical beam theory (CBT) assumptions are no longer valid. In CBT, a beam

---

*Keywords:* refined beam theory, Saint-Venant's solution, composite section, out-of-plane warpings, Poisson's effects, distortions, end-effects.

is practically reduced to a 1D body; nowadays, a beam must be considered as a 3D *slim* body whose cross-section can warp in and out-of its plane. Furthermore, a general beam theory has to account for the shape of the cross-section, the spatial arrangement of the materials and their anisotropy and must, at least, lead to an acceptable approximation of the 3D stress state in each material, which is fundamental for a composite beam.

This is the objective of the present beam theory which refers to the extended 3D SV's solution established by Iesan [1976] for an arbitrary composite cross-section. This theory is the result of a work initiated more than 10 years ago. It started offering low cost numerical methods [El Fatmi and Zenzri 2002; 2004] to compute the extended 3D SV's solution as expressed by Ladevèze and Simmonds [1998] in the framework of the *exact* beam theory. More recently a first formulation of a composite beam theory based on SV's results have been proposed [El Fatmi and Ghazouani 2011a; 2011b] but it was limited to symmetric section and particular orthotropic materials. The present work, which could be seen as a large extension of this first formulation, deals with an arbitrary homogeneous/composite cross-section. It is worth noting that this beam theory is free from all the classical assumptions and no homogenization step is needed for the composite case.

The accuracy of a beam model depends on its aptitude to capture the behavior associated with the two small dimensions eliminated in the final 1D beam analysis. From the literature surrounding the development of (1D) beam theories, three important approaches can be identified:

- beam theories based on kinematic (and static) assumptions using some engineering experience or intuition;
- beam theories based on the asymptotic expansion of the 3D solution, using small parameter(s) inherent to the beam features;
- the so-called one-dimensional beam-like theory which derives from the 3D Saint-Venant (SV) solution of SV's problem.

These different approaches have been discussed in [El Fatmi and Ghazouani 2011a] and we will not take the same (one can also see the interesting review on classical and advanced beam theories of [Carrera et al. 2011]). However, the beam theory proposed here being completely based on 3D SV's solution, this approach deserves some attention again.

Established first for homogeneous and isotropic section, SV's solution have been extended by Iesan [1976] to any composite section wherein each material is anisotropic and where the beam is also subjected to any uniform lateral loading. 3D SV's solution has always been a reference for the development of beam theories, and now even more since its extension to any composite sections [Giovotto et al. 1983; Ladevèze and Simmonds 1998; Dong et al. 2001; El Fatmi and Ghazouani 2011a; Yu et al. 2012; Genoese et al. 2014a]. This is due to the status and the asymptotic nature of SV's solution, as well as to the sectional mechanical characteristics it provides [Ladevèze and Simmonds 1998; El Fatmi and Zenzri 2002; Yu et al. 2012; Blasques 2012; El Fatmi 2012; Genoese et al. 2014a]. SV's solution, SV's principle, and SV's end-effects are redundant key-words in the literature around SV's problem for which the main results need here to be recalled.

Because it describes the exact 3D solution in the interior area of the beam, 3D SV's solution (also called central solution) reflects the real mechanical behavior of the section that results from its shape

and its materials. It is worth noting that an important set of sectional quantities can be extracted from the computation of 3D SV's solution [El Fatmi and Ghazouani 2011a; 2011b; Yu et al. 2012; Blasques 2012; El Fatmi 2012]; these quantities are:

- the canonical sectional stress fields  $\sigma_{sv}^i$ , that correspond to each one of the six cross-sectional stresses (the shear forces, the axial force, the torsional moment, the bending moments);
- the sectional out-of plane warping  $W_{sv}^i$ , and the sectional Poisson's effects  $\Pi_{sv}^i$  related to each one the 6 cross-sectional stresses;
- the structural sectional stiffness  $6 \times 6$  matrix  $\Gamma_{sv}$  wherein the off-diagonal terms reflect the *coupling effects* (between bending, torsion and tension) that can occur for an arbitrary composite section.

The existence of the sectional properties are mainly due to two important mathematical properties of SV's solution; this one is polynomial with respect to the beam axis and is a linear function of the (six) cross-sectional stresses. Using these properties, Berdichevsky [1979] has shown that 3D SV's solution can be split<sup>1</sup> into a set of 2D problems on the cross-section and a set of 1D equations that defines a beam-like theory (denoted here by SVBT). This splitting has been later used in several works to compute SV's solution using a 2D finite element technique, where only the section has to be discretized [Giovotto et al. 1983; El Fatmi and Zenzri 2002; 2004; Alpdogan et al. 2010; Blasques 2012; El Fatmi 2012; Genoese et al. 2014b]. Recently, using different numerical methods, software has even been developed as variational asymptotic beam section analysis (VABS) [Yu et al. 2012], beam cross-section analysis software (BECAS) [Blasques 2012], or composite section and beam analysis (CSection, a part of CSB) [El Fatmi 2012] to provide, for any section defined by its 2D geometry and its material(s), all its sectional characteristics ( $\sigma_{sv}^i$ ,  $W_{sv}^i$ ,  $\Pi_{sv}^i$ ,  $\Gamma_{sv}$ ).

Besides, concerning the end-effects, SV's Principle is usually taken to mean that these effects vanish closely to the loaded ends. In many cases, this is not true; see [Toupin 1965] for counter examples, and also the end-effects analysis of [Horgan and Simmonds 1991; 1994] and [Volovoi et al. 1999] when strongly anisotropic materials and/or thin-walled open profiles are involved. For such beams, end-effects can persist over distances comparable to the beam length, and even dominate the structural beam behavior; in that case SV's solution may no longer be valid to describe the elastic solution in the interior part of the beam.

The most famous case deals with the torsion of a cantilever open thin-walled profile (Figure 1(a)) for which the built-in effects (characterized here by a distance  $d$ ) can reach the loaded end. In that case, SV's solution is no longer valid to describe the solution in the interior part of the beam. This leads to a structural mechanical behavior for the beam significantly different from that predicted by (1D) SVBT's torsion; in that case one has to resort to the nonuniform torsion of [Vlasov 1959] which accounts for the restrained warping right to the built-in section.

Let's use this example to also show that, unlike conventional beam theories that distinguish compact and walled (and even thin or thick, open or closed) sections, no distinction should be done for a composite section. Indeed, consider the rectangular *compact* composite section shown in (Figure 1(c)), where both materials are isotropic but with different elastic Young's moduli  $E_1$  and  $E_2$ . When  $E_1 = E_2$ , the section

<sup>1</sup>One could find a link with the proper generalized decomposition (PGD) method [Polit et al. 2015], but it is worth noting that this decomposition is here an exact mathematical property of 3D SV's solution.

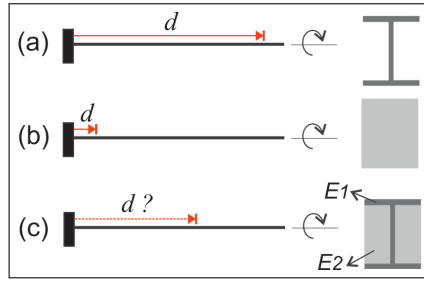


**Figure 1.** Built-in effects for cantilever beams subjected to tip torsion.

becomes a compact homogeneous section, and one can show that the built-in effect ( $d$ ) remains close to the built-in section (Figure 1(b)), SV's solution is valid in the interior area of the beam and SVBT's torsion correctly describes the structural behavior of the beam. In contrast, when  $E_1 \gg E_2$ , the beam behavior becomes similar to that of an open profile. It is here clear that the built-in effect, for this composite section, may spread over a distance  $d$  that depends on the material contrast  $E_1/E_2$  which may significantly influence the structural behavior of the beam.

What to learn from this example? Moving away from the end sections, the 3D solution tends asymptotically towards SV's solution. The *end-effects* depend on the whole nature of the cross-section and the boundary conditions, and are not necessary *confined* close to the end sections but can significantly *spread* in the interior area of the beam. In particular, for open profile or/and strongly anisotropic composite section, such end-effects may dominate the global elastic behavior of the beam. For such beams, it is then important to refine classical beam theories (and even SVBT) by incorporating, at least, the most influential end-effects. Thus, for a really general beam theory, no distinction about the kind of section has to be done. The behavior of a section is due to its whole *nature*: shape and material(s).

To improve the prediction of the classical beam theories which assume a rigid body motion of the cross-section, the so-called *higher order beam theories* are built on displacement models that allow some deformation of the section. In literature, some refined beam theories are based on a mathematical modeling of the displacement field and others, more physical, are based on a modeling that account for the cross-section nature.

As mathematical modeling, a significant contribution is the Carrera unified formulation (CUF) proposed in [Carrera and Giunta 2010]. In CUF, different  $N$ -order beam models can be developed using the same unified displacement field expression. Let  $(x, y)$  and  $z$  be the coordinates of the cross-section and the beam axis, respectively. The displacement model is written as an expansion of generic functions,  $F_\tau$ ,

$$\mathbf{u}(x, y, z) = \sum_{\tau=1}^M F_\tau(x, y) \mathbf{u}_\tau(z), \quad (1)$$

where  $M$  is the number of terms of the expansion,  $F_\tau$  the base functions that model the kinematic of the cross-section and  $\mathbf{u}_\tau$  the displacement vector. A common choice is the use of a Taylor-like  $x^i y^j$ -polynomial expansion (where  $i$  and  $j$  are integer such as  $0 \leq (i + j) \leq N$ ); in that case, one can show that the total number of displacement variables (or degrees of freedom) is given by  $[3(N + 1)(N + 2)/2]$  for an  $N$ -order beam theory. CUF, allows, a priori, to deal with an arbitrary cross-section. However, this

approach remains  $N$ -dependent and, in practice, the choice of  $N$  is not so evident because it depends on the cross-section complexity and the beam problem to solve. One can find a CUF presentation and several applications in [Carrera et al. 2015] and also a software using CUF, named MUL2, on the website [mul2.com](http://mul2.com).

In the other modeling way, more physical, the displacement field is written as

$$\xi(\mathbf{u}, \boldsymbol{\omega}, \{\eta\}) = \underbrace{\mathbf{u}(z) + \boldsymbol{\omega}(z) \wedge \mathbf{X}}_{\text{rigid motion of the section}} + \overbrace{\sum_{k=1}^n \eta_k(z) \mathbf{M}^k(x, y)}^{\text{enrichment}}, \quad (2)$$

where  $(\mathbf{u}, \boldsymbol{\omega})$  are the cross-sectional displacement (translation and rotation),  $\mathbf{X}$  the in-section vector position, and  $\{\eta\}$  a set of  $\eta_k$  control parameters of the sectional displacement modes  $\mathbf{M}^k$  which are supposed to be known. The objective of such models is to allow and control some sectional displacement modes to better satisfy the boundary conditions, which *could capture* some *end-effects*. This approach requires, as a first step, a *cross-section analysis* to determine the set  $\{\mathbf{M}^k\}$  of sectional modes to be used in the enrichment part of the displacement model. However, this way leads to a beam theory that *really fit* the cross-section, and hence the beam problem, if the set  $\{\mathbf{M}^k\}$  is sufficiently representative of the cross-section mechanics.

The pioneers of such theories are Benscoter [1954] and Vlasov [1959], who deal with the torsion of thin-walled profiles using as sectional mode an approximation of the SV-torsional out-of plane warping of the section. Later, both theories have been extended (or generalized) to different shapes of homogeneous sections and also adapted to some composite sections [Loughlan and Ata 1998; Kim and White 1997; Roberts and Al-Ubaidi 2001; Ferrero et al. 2001; Lee and Lee 2004; Yu et al. 2005; Kim et al. 2006; Pluzsik and Kollar 2006; Jung et al. 2007; Sapountzakis and Mocos 2007].

A significant contribution, even if limited to thin open/closed profiles, is given by the generalized beam theory (GBT) initiated by Schardt [1994] and currently developed by Camotim, Silvestre and their colleagues [Camotim et al. 2006; Silvestre et al. 2011; Bebiano et al. 2015]. GBT is a beam theory including, as sectional modes, out-of plane warpings and distortions. In GBT cross-section analysis step, the section is reduced to a piecewise description of its contour from which the computation of the sectional modes is done; one can find a description of this procedure in [Camotim et al. 2007] or in the manual of the software GBTUL (<http://www.civil.ist.utl.pt/gbt/>) based on GBT computations.

Another solution, available for an arbitrary cross-section, is to refer to the extended 3D SV's solution. Indeed, the set of sectional modes  $\{\mathbf{W}_{sv}^i, \boldsymbol{\Pi}_{sv}^i\}$  introduced above and that can be extracted from the computation of the correspondent SV's solution is particularly indicated<sup>2</sup> to reflect the cross-section mechanics, taking into account its shape and material(s). Using this way that refers to 3D SV's solution I proposed in [El Fatmi 2007a; 2007b; 2007c] for homogeneous beams a general nonuniform warping theory including as sectional modes the three SV out-of plane warpings  $\{\mathbf{W}_{sv}^k, i = 1, \dots, 3\}$  related to the two shear forces and the torsional moment; its enrichment displacement part is written  $\sum_{k=1}^3 \eta_k(z) \mathbf{W}_{sv}^k(x, y)$ . Later this work has been extended in [El Fatmi and Ghazouani 2011a] to composite beams, including also, as in

<sup>2</sup>Vlasov and Benscoter models constitute examples that refer to SV's solution, using as its unique sectional mode an approximation of the SV-torsional out-of plane warping.

plane deformation, the SV sectional Poisson's effects leading to the following displacement model

$$\xi(\mathbf{u}, \boldsymbol{\omega}, \{\alpha\}, \{\beta\}) = \mathbf{u}(z) + \boldsymbol{\omega}(z) \wedge \mathbf{X} + \sum_{i=1}^3 \alpha_i(z) \boldsymbol{\Pi}_{sv}^i(x, y) + \sum_{j=1}^3 \beta_j(z) \mathbf{W}_{sv}^j(x, y), \quad (3)$$

where  $\boldsymbol{\Pi}_{sv}^i$  are the sectional Poisson's effects related to the axial force and the two bending moments. However, the correspondent beam theory was limited to  $x$ - $y$ -symmetric sections made of orthotropic materials for which the principal material coordinates coincide with those of the beam (this kind of cross-section will be denoted by  $so$ -CS). Except the limitation<sup>3</sup> to  $so$ -CS, the displacement model (Equation (3)) has the advantage to lead to a refined beam theory (RBT) adapted to the section nature. This RBT built on SV's solution has been applied [El Fatmi and Ghazouani 2011b] to analyze the built-in effects influence on the structural behavior of end-loaded cantilever beams. The results, obtained for a representative set of  $so$ -CS, showed that the beam theory is able to describe the built-in effects, and hence their influence on the structural behavior of the beam. Moreover, moving away from the built-in section, the results (3D displacements and stresses) tend towards 3D SV's solution in the interior part of the beam, which is expected for a beam model built on 3D SV's solution.

In contrast with this beam model (Equation (3)) where the unknowns are only the kinematic parameters  $\eta_k$  (or  $\alpha_k$  and  $\beta_k$ ), an alternative way has been proposed by [Genoese et al. 2014a; 2014b] where the beam theory is obtained on the basis of a mixed Hellinger–Reissner principle by defining the static and the kinematics on the basis of stresses and displacements that refers to SV's solution: the kinematic description uses the six SV's sectional modes (as in (3)) and the stress field is evaluated as the sum of the contribution due to the central solution (or SV's solution) and to the six sectional modes.

The present refined beam theory (denoted RBT/SV) is a large extension of the RBT proposed in [El Fatmi and Ghazouani 2011a], also built on SV's solution, but valid for an arbitrary cross-section: compact or walled, mono or multicellular, thin or thick, symmetric or not, homogeneous or composite and each material may be fully anisotropic and free oriented. For that aim, the enrichment of the displacement model will not be limited to the (SV) sectional out-of plane warpings and the (SV) sectional Poisson's effects but introduces also some sectional distortion modes (denoted by  $\mathbf{D}^j$ ,  $j = (1, \dots, p)$ ); these latter are fundamental to help describe the mechanical behavior of thin/thick-walled profiles (Figure 2), but also some strongly contrasted composite beams (see the example of Figure 1(c)). There are different ways to choose the sectional distortions [Silvestre et al. 2011; Basaglia et al. 2011; Genoese et al. 2014b]; in the present RBT/SV,  $\mathbf{D}^j$  are also be derived from SV's solution. RBT/SV displacement model is then defined by (2) where all the sectional modes  $\mathbf{M}^k$  that express the enrichment part are extracted from SV's solution:  $\mathbf{M}^k = \{\boldsymbol{\Pi}_{sv}^i, \mathbf{W}_{sv}^i, \mathbf{D}_{sv}^j; i = (1, \dots, 6) \text{ and } j = (1, \dots, p)\}$ .

To solve a beam problem using RBT/SV, two steps are needed. The first step (the cross-section analysis) has to determine the sectional modes; this is achieved using an upgraded version of the numerical

<sup>3</sup>It is shown in [El Fatmi and Zenzri 2002], for this particular case of cross section, that the Poisson's effects are only due to the axial force and the bending moments, the out-of-plane warpings are only due to the torsional moment and the shear forces, and no elastic coupling is present in the structural behavior of the correspondent beam. For arbitrary composite beam, several elastic couplings between extensional, flexural and torsional deformations may occur [Chandra et al. 1990; Chandra and Chopra 1991; Rand 1998; 2000; Rappel and Rand 2000; Volovoi et al. 2001; El Fatmi and Zenzri 2002; 2004] and one can show that each one of the six cross-sectional stresses may lead to a Poisson's effect and an out-of plane warping (see the case the laminated section in Figure 12). Therefore, the choice of  $so$ -CS makes it possible to avoid the elastic couplings.

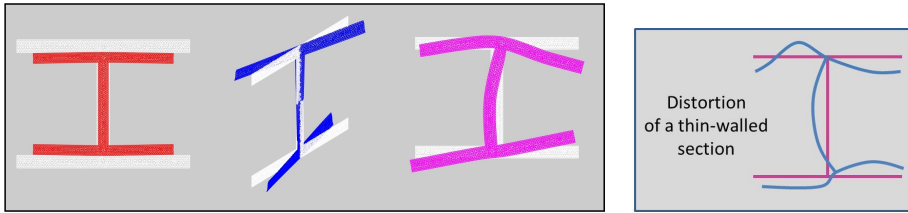


**Figure 2.** Left side: examples of a Poisson's effect, an out-of-plane warping and a distortion for an I-section. Right side: an arbitrary distortion.

Matlab tool, named CSection, I recently developed [El Fatmi 2012]. The second step uses these sectional modes to generate the correspondent beam theory and to solve the beam problem; for this step a second numerical Matlab tool, named CBeam, has been developed.

In the present paper, the first section recalls the main properties of 3D SV's solution needed for the development of the beam theory. The second section describes how the (SV) sectional modes can be extracted from SV's solution. Then, in the third section, starting from the displacement model, the corresponding beam theory is established and discussed. The numerical implementation of RBT/SV and the numerical tools CSection and CBeam are presented in the fourth section. Finally, using RBT/SV, the last section is devoted to the computations of a significant set of homogeneous and composite beams. To clearly show the accuracy of the beam model and the numerical tools<sup>4</sup> CSection and CBeam that come with it, the 1D/3D results focus on the critical points as the shear force effect in the 1D structural behavior of the beam and the 3D stress fields in the interior area of the beam and close to the ends. 1D/3D RBT/SV results are compared to 1D/3D SV's solution and to the those provided by full 3D-FEM computations, using the finite element code Abaqus.

## 2. The extended Saint-Venant's problem and solution

One can find in [El Fatmi and Zenri 2002; 2004; El Fatmi and Ghazouani 2011a; El Fatmi 2012] details about the 3D SV's solution and its properties; in this section we just recall the reference problem and the general expression of the correspondent 3D SV's solution<sup>5</sup> and some important properties. Indeed, this solution is here fundamental to extract the sectional displacement modes that will be used to formulate the beam theory.

**2A. The reference beam problem.** SV's problem is a 3D equilibrium elastic problem Figure 3. The composite beam is along the  $z$  axis and occupies a prismatic domain  $\Omega$  of cross-section  $S$  independent of  $z$  and length  $L$ .  $S_{\text{lat}}$  is the lateral surface,  $S_0$  and  $S_L$  are the end sections. A point of the beam is marked  $P = zz + \mathbf{X}$  where  $\mathbf{X}$  belongs to  $S$ . The materials constituting the beam are linear elastic, anisotropic and perfectly bonded together; the elastic tensor field denoted by  $\mathbf{K}$  is  $z$ -constant (vectors and tensors are noted in boldface characters).

<sup>4</sup>CSection and CBeam can be used as Matlab tools. An evaluation version of CSection and CBeam can be obtained from the author upon email.

<sup>5</sup>Here, the SV problem is not the original one established for homogeneous and isotropic section and due to Saint-Venant, but that of [Iesan 1976] extended to composite section and a lateral uniform loading.

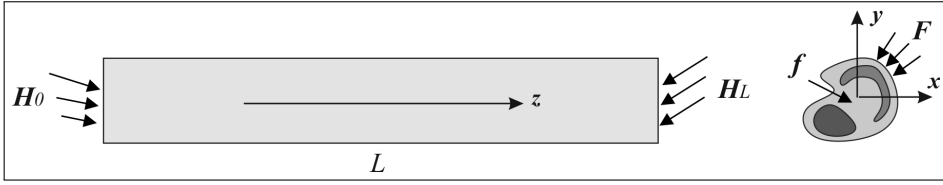


**Figure 3.** The extended Saint-Venant’s problem.

The beam is in equilibrium under a body force density  $f$  on  $\Omega$ , and surface force densities  $F$ ,  $H_0$  and  $H_L$  on  $S_{lat}$ ,  $S_0$  and  $S_L$ , respectively; the densities  $f$  and  $F$  are supposed  $z$ -constant. The equations of the linearized equilibrium are

$$\begin{aligned} \operatorname{div} \boldsymbol{\sigma} + \mathbf{f} &= \mathbf{0} && \text{in } \Omega, \\ \boldsymbol{\varepsilon}(\boldsymbol{\xi}) &= \frac{1}{2}(\nabla^t \boldsymbol{\xi} + \nabla \boldsymbol{\xi}) && \text{in } \Omega, \\ \boldsymbol{\sigma} &= \mathbf{K} : \boldsymbol{\varepsilon}(\boldsymbol{\xi}) && \text{in } \Omega, \\ \boldsymbol{\sigma} \cdot \mathbf{n} &= \mathbf{F} && \text{on } S_{lat}, \end{aligned} \tag{4}$$

$$\begin{aligned} \boldsymbol{\sigma} \cdot (-\mathbf{z}) &= \mathbf{H}_0 && \text{on } S_0, \\ \boldsymbol{\sigma} \cdot \mathbf{z} &= \mathbf{H}_L && \text{on } S_L, \end{aligned} \tag{5}$$

where  $\boldsymbol{\varepsilon}(\boldsymbol{\xi})$  is the strain tensor associated to the displacement field  $\boldsymbol{\xi}$ ;  $\nabla$ ,  $(\cdot)^t$  and  $(:)$  denote the gradient, the transpose and the double contraction operators, respectively;  $\boldsymbol{\sigma}$  is the stress tensor and  $\mathbf{n}$  is the unit vector that is normal and external to  $S_{lat}$ .

**2B. 3D SV’s solution.** 3D SV’s solution is the unique ( $z$ -polynomial) solution that exactly satisfies (4) and satisfies the boundary conditions (5) only in term of resultant (force and moment). To express hereafter SV’s solution, we introduce the forces and moments related to  $H_0$  and  $H_L$ :

$$[\mathbf{F}_0, \mathbf{C}_0] = \int_{S_0} [\mathbf{H}_0, \mathbf{X} \wedge \mathbf{H}_0] dS, \quad [\mathbf{F}_L, \mathbf{C}_L] = \int_{S_L} [\mathbf{H}_L, \mathbf{X} \wedge \mathbf{H}_L] dS, \tag{6}$$

and the classical cross-sectional stresses  $[\mathbf{R}, \mathbf{M}]$  defined by

$$\mathbf{R} = \int_S (\boldsymbol{\sigma} \cdot \mathbf{z}) dS = \begin{bmatrix} T_x \\ T_y \\ N \end{bmatrix}, \quad \mathbf{M} = \int_S (\mathbf{X} \wedge \boldsymbol{\sigma} \cdot \mathbf{z}) dS = \begin{bmatrix} M_x \\ M_y \\ M_t \end{bmatrix}, \tag{7}$$

where the six components are the 6 classical internal forces  $[T_x, T_y, N, M_x, M_y, M_t]$ : the shear forces, the axial force, the bending moments and the torsional moment, respectively.

**2B1.** *Case without a lateral loading.* In this case, the loading is reduced to  $[\mathbf{H}_0, \mathbf{H}_L]$  and 3D SV's solution is given by

$$\xi_{sv}(x, y, z) = \mathbf{u}(z) + \boldsymbol{\omega}(z) \wedge \mathbf{X} + \sum_{i=1}^6 F_i(z) \mathbf{U}_{sv}^i(x, y), \quad (8)$$

$$\boldsymbol{\sigma}_{sv}(x, y, z) = \sum_{i=1}^6 F_i(z) \boldsymbol{\sigma}_{sv}^i(x, y), \quad (9)$$

where  $F_i$  is one of the six internal forces  $\{T_x, T_y, N, M_x, M_y, M_t\}$ . In these expressions, the cross-sectional displacement  $[\mathbf{u}, \boldsymbol{\omega}]$  and the cross-sectional stresses  $[\mathbf{R}, \mathbf{M}]$  are solution of the following set<sup>6</sup> of 1D equations:

$$\begin{aligned} \mathbf{R}' &= \mathbf{0}, \\ \mathbf{M}' + \mathbf{z} \wedge \mathbf{R} &= \mathbf{0}, \\ \begin{bmatrix} \boldsymbol{\gamma} \\ \boldsymbol{\chi} \end{bmatrix} &= \begin{bmatrix} \mathbf{u}' + \mathbf{z} \wedge \boldsymbol{\omega} \\ \boldsymbol{\omega}' \end{bmatrix} = \mathbf{\Lambda}_{sv} \begin{bmatrix} \mathbf{R} \\ \mathbf{M} \end{bmatrix}, \\ [\mathbf{R}, \mathbf{M}]_{z=0} &= [-\mathbf{F}_0, -\mathbf{C}_0], \\ [\mathbf{R}, \mathbf{M}]_{z=L} &= [\mathbf{F}_L, \mathbf{C}_L], \end{aligned} \quad (10)$$

where  $(\cdot)'$  denotes the derivative with respect to  $z$ . Besides, the  $6 \times 6$  compliance matrix  $\mathbf{\Lambda}_{sv}$ , which defines the structural 1D behavior of the beam, is related to the elasticity tensor  $\mathbf{K}$  by

$$\mathbf{\Lambda}_{sv} = [\lambda_{ij}], \quad \lambda_{ij} = \int_S \boldsymbol{\sigma}_{sv}^i(x, y) : \mathbf{K}^{-1}(x, y) : \boldsymbol{\sigma}_{sv}^j(x, y) dS. \quad (11)$$

**Remark 2.1.** In 3D SV's solution,  $\mathbf{U}_{sv}^i$ ,  $\boldsymbol{\sigma}_{sv}^i$  and  $\mathbf{\Lambda}_{sv}$  don't depend on the beam problem, but only on the section nature (shape and materials). For a given cross-section defined by its 2D geometry and its material(s), these (SV) sectional quantities can be determined once and for all. In that case, for a given beam problem, they can be used to easily obtain the correspondent 3D SV solution; for that aim, two steps are needed:

- (i)  $\mathbf{\Lambda}_{sv}$  is used to solve the 1D problem (10) to obtain the correspondent 1D solution  $[\mathbf{u}, \boldsymbol{\omega}, \mathbf{R}, \mathbf{M}]$ ;
- (ii) then,  $[\mathbf{U}_{sv}^i, \boldsymbol{\sigma}_{sv}^i]$  are used to immediately express the 3D SV's solution according to (8) and (9).

**2B2.** *Case with a lateral loading.* If a  $z$ -uniform lateral loading  $[\mathbf{f}, \mathbf{F}]$  is added to  $[\mathbf{H}_0, \mathbf{H}_L]$ , the expression of SV's changes<sup>7</sup> and, in particular, the expression of the displacement becomes

$$\xi_{sv}(x, y, z) = \mathbf{u}(z) + \boldsymbol{\omega}(z) \wedge \mathbf{X} + \sum_{i=1}^6 F_i(z) \mathbf{U}_{sv}^i(x, y) + \mathbf{D}_{sv}(x, y), \quad (12)$$

<sup>6</sup>These 1D equations define the SV beam-like theory (SVBT).

<sup>7</sup>For more details, see [Ladevèze and Simmonds 1998; El Fatmi and Zenzri 2002; 2004].

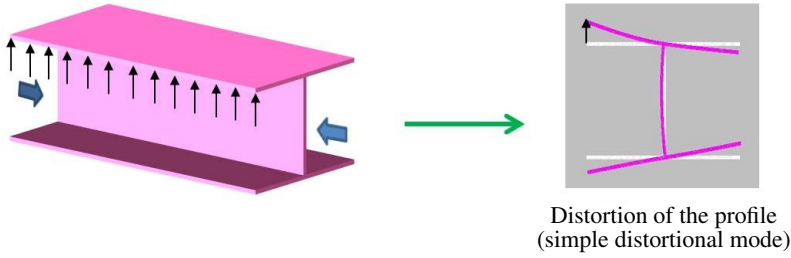


**Figure 4.** The sectional distortion  $D_{sv}$  related to the uniform lateral load.

where the vector  $D_{sv}$ , which is proportional to  $[f, F]$ , depends only on the section nature (shape and materials) and the kind of  $[f, F]$  loading. Therefore, for a given uniform lateral loading  $[f, F]$ ,  $D_{sv}$  can be determined once and for all [El Fatmi 2012].

### 3. The sectional displacement modes

Three kinds of sectional modes are extracted from the SV displacement expressions (8) and (12): the Poisson's effects and the out of plane warpings related to each one of the six internal forces and several sectional distortions. An example of each kind of mode is given left side of Figure 2. For a given section (shape and materials), all these SV sectional modes will be provided by the numerical tool CSection [El Fatmi 2012] which has been upgraded for the present work (a quick presentation of CSection is done in section-5A).

**3A. Sectional Poisson's effects and out-of plane warpings.** The expression of the 3D SV displacement (Equation (8)) may be seen as the contribution of two parts:

- $[u(z) + \omega(z) \wedge X]$ , which reflects the rigid motion of the section,
- $[\sum_{i=1}^6 F_i(z) U_{sv}^i(x, y)]$ , which reflects the contribution of each internal forces to the deformation of the section.

Because  $U_{sv}^i$  depend only on the section nature (shape and materials), they are viewed as sectional deformation modes. Moreover, each  $U_{sv}^i$  can be split into two parts:

- $W_{sv}^i = (U_{sv}^i \cdot z) z$ , the out of plane warping,
- $\Pi_{sv}^i = U_{sv}^i - W_{sv}^i$ , the in plane warping that can be related to the Poisson's effect.

The set of  $\{\Pi_{sv}^i, W_{sv}^i; i = 1, \dots, 6\}$  define a first set of deformation modes for the section.

**Remark 3.1.** For homogeneous and isotropic sections and even for *so*-CS introduced above, Poisson's effects are only due to the axial force and the bending moments, and the out-of plane warpings are only due to the shear forces and the torsional moment. However, for an arbitrary composite section each one of the six internal forces may contribute<sup>8</sup> to the Poisson's effects and to the out-of-plane warpings; Figure 12 shows these sectional modes for a laminated section (symmetric or antisymmetric) using anisotropic layers.

<sup>8</sup>This is intimately associated to the elastic couplings between extensional, flexural and torsional deformations that can occur for an arbitrary cross-section.

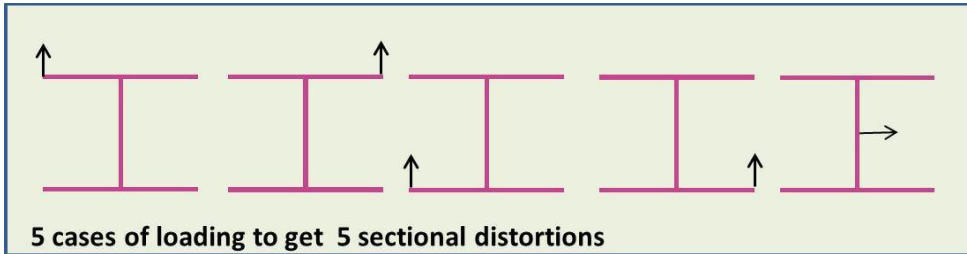


**Figure 5.** Example of uniform lateral loads for the I-section.

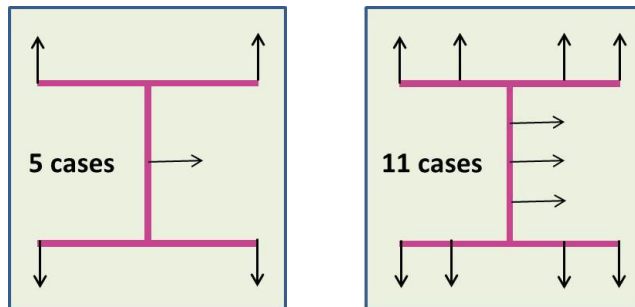


**Figure 6.** Different load cases (5 and 11) for the I-section.

**3B. Sectional distortions.** An arbitrary sectional distortion (right side of Figure 2) may be approximated by the combination of  $p$  simple distortional modes. The way used to identify a simple distortional mode is the following (Figure 4): we consider a SV problem with a particular uniform and lateral load  $F$  and we extract from the corresponding displacement SV solution (Equation (12)), the vector  $D_{sv}$ . The later which contributes to the displacement and which is due to the presence (and the location) of the lateral load is viewed as a distortional mode; for instance, see the result obtained for  $D_{sv}$  in the right-side of Figure 4. To obtain  $p$  simple distortional modes, one has to consider (separately)  $p$  cases of lateral loads. For example, five uniform lateral loads<sup>9</sup> may be considered to compute (separately) five simple distortion modes for the I-section (Figure 5), each case is related to a uniform lateral load. These five cases can be summarized on the cross-section (left side of Figure 6). However, one could choose a larger number of cases, for example the 11 cases presented in the right side of Figure 6. Figure 7 shows the 11 simple sectional distortion modes (computed by CSection) that correspond to the 11 load cases. This procedure is not automatic and need a little experience: dealing with a thin-walled section, each case of load is chosen to *cause the local bending* of a branch, or a part of the section contour easy to deform.

**Remark 3.2.** Other sectional modes are being investigated:

- The procedure to generate the distortions is not automatic and requires some experience. An alternative solution (more systematic) is to choose the first natural in-plane modes of vibration of the section.

<sup>9</sup>For this particular section, thanks to the symmetries, these loads can of course be theoretically reduced to one vertical load and the horizontal one. However this example is here given only to show how the loads can be chosen.

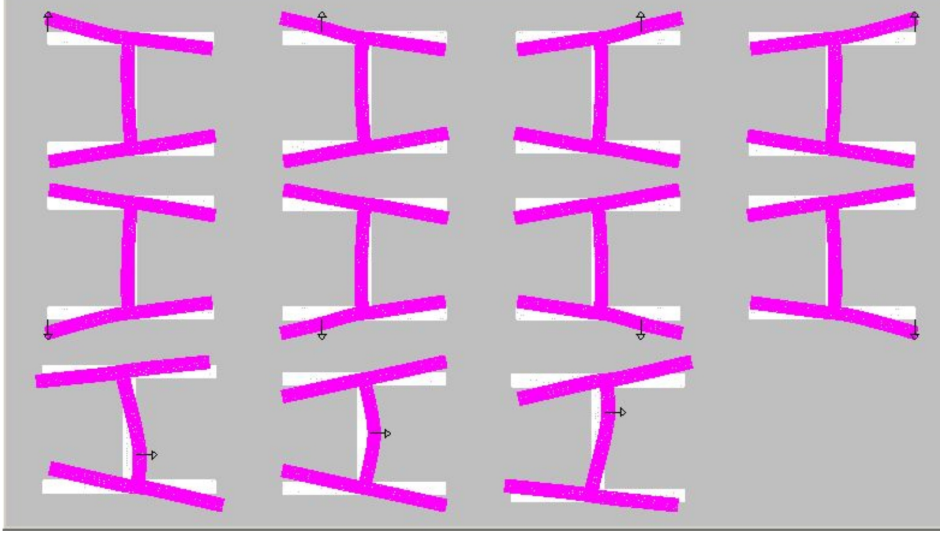


**Figure 7.** The 11 sectional distortions of the I-section.

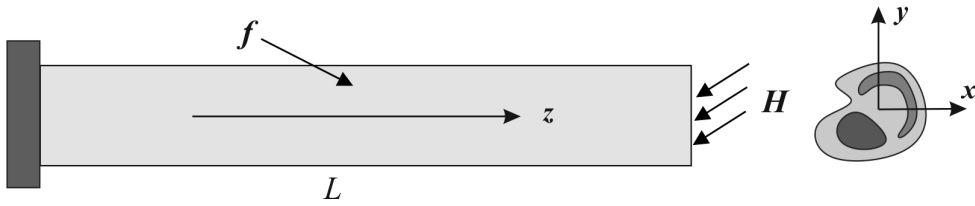


**Figure 8.** Cantilever composite beam subjected to a body force and a tip traction.

- Concerning the out of plane warpings, they are here limited to those extracted from SV’s solution and they might be considered as the most important ones. However, for the case which cannot be described with SV’s modes, an enrichment may also be done using the first out-of plane natural vibrations of the section.

To allow these investigations, the software CBeam presented in Section 5B has been designed to run regardless of the number of sectional modes provided for the section.

#### 4. The refined beam theory built on SV’s solution

To derive the equations that govern the beam theory (RBT/SV), we consider just for convenience, the cantilever composite beam (Figure 8) subjected to a body loading  $f$  and a traction  $H$  acting on  $S_L$ .

**4A. Kinematical modeling.** The RBT/SV displacement model is given by

$$\xi_{\text{RBT/SV}}(x, y, z) = \xi(\mathbf{u}, \boldsymbol{\omega}, \{\eta\}) = \mathbf{u}(z) + \boldsymbol{\omega}(z) \wedge \mathbf{X} + \eta_k(z) \mathbf{M}^k(x, y), \tag{13}$$

where  $(\eta_k(z)\mathbf{M}^k(x, y))$  is here a sum using the repeated indices convention with  $k \in \{1, \dots, n\}$ . In RBT/SV model, the sectional modes  $\mathbf{M}^k$  are the *own* modes of the section that *derive* from the correspondent 3D SV's solution. The set of sectional modes  $\mathbf{M}^k$  is given by all the available sectional modes for the cross-section:

- $\mathbf{W}_{sv}^i$ , the sectional out of plane warping ( $i \in \{1, \dots, 6\}$ ),
- $\mathbf{\Pi}_{sv}^i$ , the sectional Poisson's effects ( $i \in \{1, \dots, 6\}$ ),
- $\mathbf{D}_{sv}^j$ , a set of sectional distortion modes ( $j \in \{1, \dots, p\}$ ).

The beam theory associated with this displacement model, parametrized by  $(\mathbf{u}, \boldsymbol{\omega}, \{\eta\})$ , is derived below thanks to the virtual work principle; however, this way being classical, only the main equations are specified and commented (for more details see, for example, [El Fatmi and Ghazouani 2011a]).

Using the matrix notation, the strain tensor components corresponding to this displacement model are

$$[\boldsymbol{\varepsilon}] = \begin{bmatrix} \varepsilon_{xx} \\ \varepsilon_{yy} \\ 2\varepsilon_{xy} \\ 2\varepsilon_{xz} \\ 2\varepsilon_{yz} \\ \varepsilon_{zz} \end{bmatrix} = \begin{bmatrix} 0 \\ 0 \\ 0 \\ \gamma_x - y\chi_z \\ \gamma_y + x\chi_z \\ \gamma_z + y\chi_x - x\chi_y \end{bmatrix} + \begin{bmatrix} \eta_k M_{x,x}^k \\ \eta_k M_{y,y}^k \\ \eta_k (M_{x,y}^k + M_{y,x}^k) \\ \eta_k M_{z,x}^k + \eta'_k M_x^k \\ \eta_k M_{z,y}^k + \eta'_k M_y^k \\ \eta'_k M_z^k \end{bmatrix}, \tag{14}$$

where  $\boldsymbol{\gamma} = \mathbf{u}' + \mathbf{z} \wedge \boldsymbol{\omega}$ ,  $\boldsymbol{\chi} = \boldsymbol{\omega}'$ , and  $(\cdot)_{,x}$  or  $(\cdot)_{,y}$  denote the derivative with respect to  $x$  or  $y$ , respectively;  $\mathbf{z}$  is the unit vector along the beam axis, as already mentioned.

**4B. Internal forces, external forces and equilibrium equations.** Let us denote by  $\hat{\boldsymbol{\xi}} = \boldsymbol{\xi}(\hat{\mathbf{u}}, \hat{\boldsymbol{\omega}}, \{\hat{\eta}\})$  a virtual displacement that satisfies the boundary conditions  $(\hat{\mathbf{u}}, \hat{\boldsymbol{\omega}}, \{\hat{\eta}\}) = (\mathbf{0}, \mathbf{0}, \{0\})$  at  $z = 0$  and  $\hat{\boldsymbol{\varepsilon}} = \boldsymbol{\varepsilon}(\hat{\boldsymbol{\xi}})$  the corresponding virtual strain tensor. The internal virtual work is

$$W_i = - \int_L \int_S \boldsymbol{\sigma} : \hat{\boldsymbol{\varepsilon}} dS dz. \tag{15}$$

Using (14),  $W_i$  takes the form

$$\begin{aligned} W_i &= - \int_L (\mathbf{R} \cdot \hat{\boldsymbol{\gamma}} + \mathbf{M} \cdot \hat{\boldsymbol{\omega}} + A^k \hat{\eta}'_k + A_s^k \hat{\eta}_k) dz \\ &= \int_L [\mathbf{R}' \cdot \hat{\mathbf{u}} + (\mathbf{M}' + \mathbf{x} \wedge \mathbf{R}) \cdot \hat{\boldsymbol{\omega}} + (A^{k'} - A_s^k) \hat{\eta}_k] dz - [\mathbf{R} \cdot \hat{\mathbf{u}} + \mathbf{M} \cdot \hat{\boldsymbol{\omega}} + A^k \hat{\eta}_k]_L, \end{aligned} \tag{16}$$

where  $(\mathbf{R}, \mathbf{M})$ , the classical cross sectional stresses, and the new (or additional) ones  $(A^k, A_s^k)$  are related to the stress tensor by

$$\mathbf{R} = \int_S \boldsymbol{\sigma} \cdot \mathbf{z} dS, \tag{17}$$

$$\mathbf{M} = \int_S (\mathbf{X} \wedge \boldsymbol{\sigma} \cdot \mathbf{z}) dS, \tag{18}$$

$$A^k = \int_S (\tau_{xz} M_x^k + \tau_{yz} M_y^k + \sigma_{zz} M_z^k) dS, \quad (19)$$

$$A_s^k = \int_S (\sigma_{xx} M_{x,x}^k + \sigma_{yy} M_{y,y}^k + \tau_{xy} (M_{x,y}^k + M_{y,x}^i) + \tau_{xz} M_{z,x}^k + \tau_{yz} M_{z,y}^k) dS, \quad (20)$$

where

$$[\sigma_{xx}, \sigma_{yy}, \tau_{xy}, \tau_{xz}, \tau_{yz}, \sigma_{zz}]$$

are the components of the stress tensor. The external virtual work is

$$W_e = \int_L \int_S \mathbf{f} \cdot \hat{\boldsymbol{\xi}} dS dz + \int_{S_L} \mathbf{H} \cdot \hat{\boldsymbol{\xi}} dS. \quad (21)$$

Using the expression of  $\hat{\boldsymbol{\xi}}$ ,  $W_e$  takes the form

$$W_e = \int_L (\mathbf{p} \cdot \hat{\mathbf{u}} + \boldsymbol{\mu} \cdot \hat{\boldsymbol{\omega}} + \kappa^k \hat{\eta}_k) dz + \mathbf{P} \cdot \hat{\mathbf{u}}_L + \mathbf{C} \cdot \hat{\boldsymbol{\omega}}_L + \mathbf{Q}^k \hat{\eta}_L^k, \quad (22)$$

where the (1D) generalized external forces  $(\mathbf{p}, \boldsymbol{\mu}, \kappa^k, \mathbf{P}, \mathbf{C}, \mathbf{Q}^k)$  are defined by

$$\begin{aligned} \mathbf{p} &= \int_S \mathbf{f} dS, & \mathbf{P} &= \int_{S_L} \mathbf{H} dS, \\ \boldsymbol{\mu} &= \int_S \mathbf{X} \wedge \mathbf{f} dS, & \mathbf{C} &= \int_{S_L} \mathbf{X} \wedge \mathbf{H} dS, \\ \kappa^k &= \int_S \mathbf{f} \cdot \mathbf{M}^k, & \mathbf{Q}^k &= \int_{S_L} \mathbf{H} \cdot \mathbf{M}^k dS, \end{aligned} \quad (23)$$

where  $(\mathbf{p}, \boldsymbol{\mu}, \mathbf{P}, \mathbf{C})$  are classical and  $(\kappa^k, \mathbf{Q}^k)$  are new (or additional) generalized external forces related to the sectional deformation modes  $\mathbf{M}^k$ . Thanks to the principle of virtual work, Equations (16) and (22) are used to provide the equilibrium equations

$$\begin{aligned} \mathbf{R}' + \mathbf{p} &= 0, \\ \mathbf{M}' + \mathbf{x} \wedge \mathbf{R} + \boldsymbol{\mu} &= 0, \\ A^{k'} - A_s^k + \kappa^k &= 0 \quad (\text{for all } k), \end{aligned} \quad (24)$$

and the boundary conditions

$$x = L, \quad (\mathbf{R}, \mathbf{M}) = (\mathbf{P}, \mathbf{C}) \quad \text{and} \quad A^k = \mathbf{Q}^k \quad (\text{for all } k). \quad (25)$$

**4C. Structural behavior.** Using matrix notation, the strain tensor can be written  $\mathcal{D}$ :

$$[\boldsymbol{\varepsilon}](x, y, z) = \mathbf{B}(x, y) \mathcal{D}(z), \quad (26)$$

with

$$\mathbf{B} = \begin{bmatrix} 0 & 0 & 0 & 0 & 0 & 0 & \dots & M_{x,x}^k & 0 & \dots \\ 0 & 0 & 0 & 0 & 0 & 0 & \dots & M_{y,y}^k & 0 & \dots \\ 0 & 0 & 0 & 0 & 0 & 0 & \dots & M_{x,y}^k + M_{y,x}^k & 0 & \dots \\ 1 & 0 & 0 & 0 & 0 & -y & \dots & M_{z,x}^k & M_x^k & \dots \\ 0 & 1 & 0 & 0 & 0 & x & \dots & M_{z,y}^k & M_y^k & \dots \\ 0 & 0 & 1 & y & -x & 0 & \dots & 0 & M_z^k & \dots \end{bmatrix}, \quad \mathcal{D} = \begin{bmatrix} \gamma_x \\ \gamma_y \\ \gamma_z \\ \chi_x \\ \chi_y \\ \chi_z \\ \vdots \\ \eta_k \\ \eta'_k \\ \vdots \end{bmatrix}, \quad (27)$$

where  $\mathcal{D}$  represents the generalized 1D strain vector. If  $\mathcal{T}$  denotes the corresponding generalized cross-sectional stress vector, the 1D elastic constitutive relation can be written  $\mathcal{T} = \mathbf{\Gamma} \mathcal{D}$  where  $\mathbf{\Gamma}$  defines the 1D structural rigidity operator

$$\begin{bmatrix} \mathbf{R} \\ \mathbf{M} \\ \vdots \\ A_s^k \\ A_k \\ \vdots \end{bmatrix} = \mathbf{\Gamma} \begin{bmatrix} \boldsymbol{\gamma} \\ \boldsymbol{\chi} \\ \vdots \\ \eta_k \\ \eta'_k \\ \vdots \end{bmatrix}. \quad (28)$$

The operator  $\mathbf{\Gamma}$  may be derived from the identification

$$\int_S ([\boldsymbol{\varepsilon}_I]^t [\mathbf{K}] [\boldsymbol{\varepsilon}_J]) dS = [\mathcal{D}_I]^t \mathbf{\Gamma} [\mathcal{D}_J], \quad (29)$$

where  $(\boldsymbol{\varepsilon}_I, \mathcal{D}_I)$  and  $(\boldsymbol{\varepsilon}_J, \mathcal{D}_J)$  are any virtual strains. Introducing the expression of the deformations (Equation (26)), we obtain the following results for  $\mathbf{\Gamma}$ :

$$\mathbf{\Gamma} = \int_S \mathbf{B}^t(x, y) [\mathbf{K}](x, y) \mathbf{B}(x, y) dS. \quad (30)$$

**4D. The RBT/SV equations.** To summarize, the displacement model  $\boldsymbol{\xi}(\mathbf{u}, \boldsymbol{\omega}, \{\eta\})$  has led to a beam theory governed by the set of 1D equations

$$\begin{aligned} \mathbf{R}' + \mathbf{p} &= 0, \\ \mathbf{M}' + \mathbf{x} \wedge \mathbf{R} + \boldsymbol{\mu} &= 0, \\ A^{k'} - A_s^k + \kappa^k &= 0 \quad (\text{for all } k), \\ \mathcal{T} &= \mathbf{\Gamma} \mathcal{D}, \end{aligned} \quad (31)$$

and, for the cantilever reference problem (Figure 8), the 1D boundary conditions are

$$\begin{aligned} x = 0, & & (\mathbf{u}, \boldsymbol{\omega}, \{\eta\}) &= (\mathbf{O}, \mathbf{O}, \{O\}), \\ x = L(\mathbf{R}, \mathbf{M}) &= (\mathbf{P}, \mathbf{C}), & A^k &= Q^k \quad (\text{for all } k). \end{aligned} \quad (32)$$

**4E. The correspondent 3D solution.** Let  $\mathbf{u}^e, \boldsymbol{\omega}^e, \{\eta^e\}$  be the 1D equilibrium solution of a beam problem using RBT/SV. Conforming to the displacement model, the correspondent 3D solution is given by the 3D displacement field

$$\boldsymbol{\xi}_{\text{RBT/SV}}^e(x, y, z) = \boldsymbol{\xi}(\mathbf{u}^e, \boldsymbol{\omega}^e, \{\eta^e\}) = \mathbf{u}^e(z) + \boldsymbol{\omega}^e(z) \wedge \mathbf{X} + \eta_k^e(z) \mathbf{M}^k(x, y), \quad (33)$$

which leads to the 3D stress tensor field

$$\boldsymbol{\sigma}_{\text{RBT/SV}}^e(x, y, z) = \mathbf{K}(x, y) : \boldsymbol{\varepsilon}(\boldsymbol{\xi}^e(x, y, z)) = [\mathbf{K}](x, y) \mathbf{B}(x, y) \mathcal{D}^e(z). \quad (34)$$

The 3D stress field may also be given with respect to the internal forces:

$$\boldsymbol{\sigma}_{\text{RBT/SV}}^e = [\mathbf{K}](x, y) \mathbf{B}(x, y) \boldsymbol{\Gamma}^{-1} \mathcal{T}^e(z). \quad (35)$$

**4F. Comments.** RBT/SV displacement model (Equation (13)), which is built on 3D SV's solution, may be seen as a model which starts from the exact 3D SV displacement form (Equation (8)), where the sectional stresses  $F_i$  are relaxed in favor of independent in-and-out warping parameters ( $\eta_k$ ). These new kinematical parameters ( $\eta_k$ ) lead, by duality, to enrich the static ones (the internal and external generalized forces) which could better satisfy the boundary conditions. Therefore, if the beam length is sufficiently large, it is expected that 3D RBT/SV solution coincide with 3D SV's solution in the interior area of the beam, and better describes the end effects (see the examples presented in Section 6C).

## 5. Numerical implementation and numerical tools

To solve a beam problem using RBT/SV, two steps are needed; each one of them is associated to a numerical tool: CSection and CBeam. CSection computes by 2D-FEM the sectional modes of the cross-section; then, CBeam, uses these sectional modes to generate systematically the correspondent beam theory (RBT/SV) and to compute by 1D-FEM the beam problem. Developed on Matlab platform as any Matlab-tool, CSection and CBeam are complementary and constitute a package named CSB (composite section and beam analysis). These numerical tools are quickly presented hereafter.

**5A. CSection to compute the sectional characteristics.** CSection [El Fatmi 2012] is a numerical tool devoted to the computation of all the sectional characteristics of an arbitrary cross-section

$$\{\boldsymbol{\Gamma}_{\text{sv}}, \boldsymbol{\sigma}_{\text{sv}}^i, \boldsymbol{\Pi}_{\text{sv}}^i, \mathbf{W}_{\text{sv}}^i (i = 1 \cdots 6), \mathbf{D}_{\text{sv}}^j (j = 1 \cdots p)\}.$$

CSection is developed conforming to the numerical method proposed by El Fatmi and Zenzri [2002]. This method consists in solving, by 2D finite elements, a set of elastic problems on the section from which all the above sectional characteristics are deduced. In the first version, the sectional modes provided by CSection were limited to the Poisson's effects and the out-of-plane warpings. For the present work, CSection has been upgraded in order to provide also a set of sectional distortions. For a given cross-section,  $n = 6 + p$  linear 2D problems are solved and the numerical cost is low considering that the  $n$  problems use the same rigidity matrix. The time needed to compute a section with 1000 elements (six-node triangles) is about a few seconds on a common PC; however, for a composite section as a laminated one, the discretization can be more important and need a little more time (for instance, the laminated cross-section presented in Section 6B has 5230 elements and its computation is about 20 seconds).

**Remark 5.1.** It is worth noting that all the characteristics provided for a section constitute a relevant set of information about the *section Mechanics* that can help section design and even predict the mechanical behavior of the beam that will result.

**5B. CBeam to compute the beam.** CBeam computes the equilibrium of a straight beam subjected to any loading and boundary conditions. CBeam solves by 1D-FEM the beam problem according to RBT/SV equations *regardless of the number*<sup>10</sup> *of sectional modes* available for the cross-section.

RBT/SV displacement model (13) uses a set of kinematical parameters  $\{\mathbf{u}, \boldsymbol{\omega}, \{\eta\}\}$  which represent  $m = 6 + n$  independent degrees of freedom (DOF) for the displacement field: three translations  $[u_x, u_y, u_z]$ , three rotations  $[\omega_x, \omega_y, \omega_z]$  and the  $\eta_k$  associated to the sectional modes available for the cross-section. In CBeam, RBT/SV equations are solved by 1D-FEM using cubic (Hermite type) interpolation (shape) functions for each one of the  $m$  DOF.

In CBeam, the loading has to be introduced in a 3D way, as it is applied and localized on the beam. The computation of the 1D sectional forces (or generalized external forces) needed by the 1D-FEM computation (as  $\kappa^k$  or  $Q^k$  in (23)) are ensured automatically by CBeam.

The displacement boundary conditions may act on each sectional parameter of the displacement model (or each DOF). For instance, for a built-in section, one has to block not only the cross-sectional displacement  $(\mathbf{u}, \boldsymbol{\omega})$  but also  $\{\eta\}$  to restrain the deformation right to the built-in section. Another interesting use is the simulation of a diaphragm placed inside a closed thin-walled profile: one may block just the in plane deformation right to the cross-section where the diaphragm is located.

In CBeam, just for comparison, two solvers are proposed: RBT/SV solver and SVBT solver. RBT/SV solver solves the beam problem using RBT/SV and SVBT solver solves the beam problem to get the correspondent 3D SV's solution<sup>11</sup> according to (8)–(10) (see Remark 2.1). Using RBT/SV solver or SVBT solver, the resolution being by 1D-FEM, the time required to solve any beam problem is really insignificant (less of one second on a common PC).

## 6. Numerical applications and results

To illustrate the efficiency of RBT/SV and the numerical tools CSection and CBeam that come with, a significant set of homogeneous and composite beams are computed, using different loads and displacement conditions. The panel of the different cross-sections and beam problems to be analyzed have been chosen to clearly show that RBT/SV is able to describe the different kinds of 3D effects related to the section nature (shape and materials), to take for account a significant part of the end effects (as those related to the restrained warpings) and to provide a good description of the structural beam behavior, even if the beam slenderness is relatively small.

The most important 1D/3D results are presented focusing on the 3D stress fields, in the interior area of the beam and close to the ends. RBT/SV results are compared to 3D SV's solution (also computed by

<sup>10</sup>For the present work, the sectional modes are those deriving from 3D SV's solution, but (in CBeam) the user is free to introduce any additional sectional mode he wants to consider, as an analytic closed form function of the section coordinates  $x$  and  $y$ . Each additional mode is associated systematically to an additional parameter ( $\eta$ ) which is viewed as a new degree of freedom for the section deformation. In CBeam, the independence of the sectional modes is systematically checked and the current solver uses a simple diagonal preconditioning to avoid the singularities of the operators.

<sup>11</sup>Of course, for SVBT solver the displacement boundary conditions act (as in classical beam theory) only on  $\mathbf{u}$  and  $\boldsymbol{\omega}$ .

Mats	$E_s = 200 \text{ GPa}$	$\nu = 0.25$	
Matc	$E_c = \{200, 100, 10, 4, 1\} \text{ GPa}$	$\nu = 0.25$	
Mat33	$E_Z = 148.00 \text{ GPa}$ $G_{XZ} = 4.40 \text{ GPa}$ $\nu_{XZ} = 0.33$	$E_X = 8.37 \text{ GPa}$ $G_{YZ} = 4.40 \text{ GPa}$ $\nu_{YZ} = 0.33$	$E_Y = 8.37 \text{ GPa}$ $G_{XY} = 2.72 \text{ GPa}$ $\nu_{XY} = 0.54$

**Table 1.** The materials.

CBeam but using SVBT-solver) and to those provided by a full 3D-FEM computation, using the finite element code Abaqus.

### 6A. The materials, the sections and the beam problems.

**6A1. The materials.** The materials are given in Table 1 where  $E$ ,  $G$  and  $\nu$  denote the Young modulus, the shear modulus and the Poisson's ratio, respectively. Mats (s as skin) and Matc (c as core) are two contrasted isotropic materials for which  $E_s/E_c$  can reach 200; Mat33 is an orthotropic<sup>12</sup> material used in [El Fatmi and Ghazouani 2011b] and chosen because its ratio  $E/G \approx 33$  is important which can significantly influence the amount of the restrained warping effect in case of torsion, even if the beam is not an open-walled profile.

**6A2. The sections.** Three homogeneous sections (H1, H2 and H3) and three composite sections (C1, C2 and C3) are considered; their dimensions are specified in Figure 9:

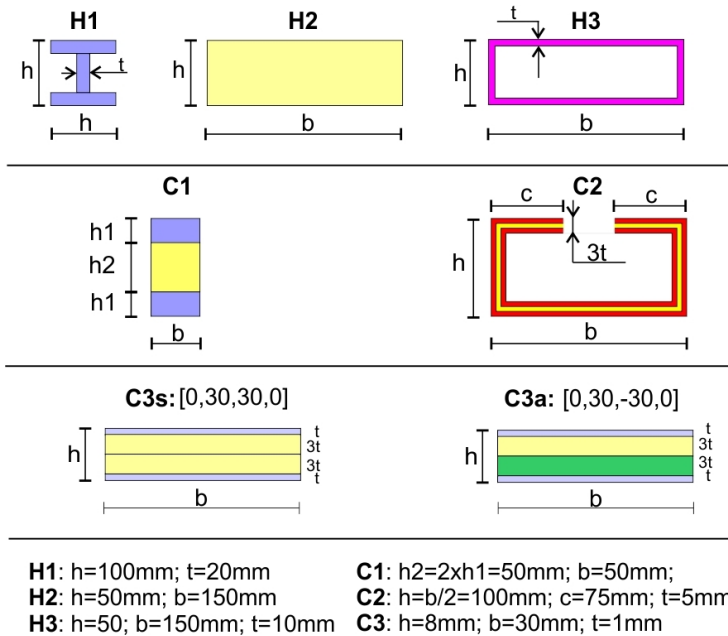


**Figure 9.** The different cross-sections and their dimensions.

<sup>12</sup> Mat33 is in fact a transversely isotropic material.

- H1 is a thick isotropic (Mats) I-section;
- H2 is a compact rectangular orthotropic (Mat33) section;
- H3 is a thin orthotropic (Mat33) box section;
- C1 is a sandwich section where the materials are isotropic (Mats, Matc) and strongly contrasted  $E_s/E_c = 200$ ;
- C2 is a nonsymmetric open-walled and sandwich section where the materials (Mats, Matc) are isotropic with  $E_s/E_c = 50$ ;
- C3 is a symmetric (C3s) or antisymmetric (C3a) laminated section using the same layers (Mat33) with  $[0, +30, +30, 0]$  and  $[0, -30, +30, 0]$  orientations, respectively.

**6A3. The beam problems.** Using the above sections, six equilibrium beam problems (Figure 10) are analyzed:

- P1: the bending-torsion of a cantilever H1-beam of length  $L = 10h$ ; the end loads are applied as indicated in Figure 10 where the magnitude of the force is  $F = 1000$  N;
- P2: the torsion of a cantilever H2-beam of length  $L = 10h$ ; the end loads are applied as indicated in Figure 10 where the magnitude of the force is  $F = 1000$  N;
- P3: the bending of a clamped-clamped H3-beam of length  $L = 10h$ ; the upper face of the beam is subjected to a pressure  $q = 10000$   $\text{Nm}^{-2}$ ;
- P4: the bending of a clamped-clamped composite C1-beam of length  $L = 20h$ ; the beam is subjected to the body force  $\mathbf{f} = \rho \mathbf{g}$  with  $g = 10$   $\text{ms}^{-2}$ ,  $\rho_s = 7500$   $\text{kgm}^{-3}$ ,  $\rho_c = 250$   $\text{kgm}^{-3}$ ;
- P5: the bending-torsion of a short ( $L/h = 7$ ) cantilever composite C2-beam subjected to a lateral traction  $q = 10000$   $\text{Nm}^{-2}$ ;
- P6: a cantilever laminated C3-beam of length  $L = 10h$  (symmetric or antisymmetric) subjected to a tension  $q = 10000$   $\text{Nm}^{-2}$ .

## 6B. Cross-section analyses.

**6B1. Sectional constants.** Tables 2 and 3 provide, for each section, the (nonzero) components of the  $6 \times 6$  rigidity matrix  $\mathbf{\Gamma}_{sv}$  related to the structural 1D behavior. Note that, as expected: no elastic coupling is present for the sections H1, H2, H3 and C1; for C2, the only off-diagonal term ( $\Gamma_{16}$ ) is due to the nonsymmetry<sup>13</sup> of the section; however the laminated composite sections C3a and C3s exhibit 2 and 3 off-diagonal terms, respectively, which reflect different elastic couplings (between extensional, flexural and torsional deformation) arising from the anisotropic nature of the layers and their stacking sequences.

**Remark 6.1.** For the sandwich section C1, one can deduce from  $\mathbf{\Gamma}_{sv}$  (computed for different ratios  $r = E_s/E_c$ ) the values of the shear coefficients  $k_y$  with respect to  $r$ . The results, given in Table 4, clearly show how much  $k_y$  can be affected when the sandwich is strongly contrasted. In such a case, it is expected to get an important shear force effect for an  $x$ -flexure of the correspondent beam (see the solution to problem P4).

<sup>13</sup>For C2, the position of the shear center  $C$ , given by CSection, is  $y_C = \mathbf{GC}$ ,  $\mathbf{y} = -9.37$  mm.

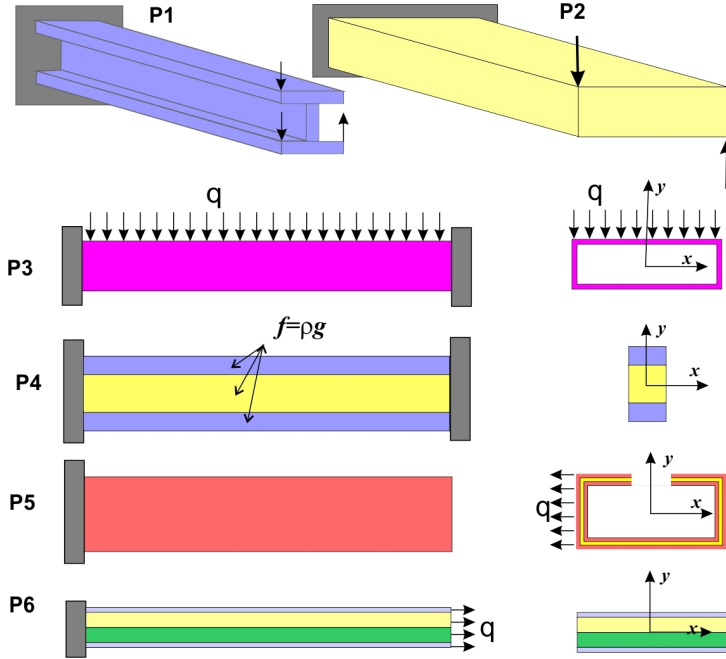


**Figure 10.** The equilibrium beam problems.

Sect.	H1	H2	H3	C1
$\Gamma_{11}$	$2.8788 \cdot 10^8$	$2.7500 \cdot 10^7$	$2.1254 \cdot 10^8$	$1.6117 \cdot 10^8$
$\Gamma_{22}$	$1.3211 \cdot 10^8$	$2.7460 \cdot 10^7$	$3.8106 \cdot 10^7$	$2.4131 \cdot 10^6$
$\Gamma_{33}$	$1.0400 \cdot 10^9$	$1.1100 \cdot 10^9$	$7.2000 \cdot 10^8$	$5.0250 \cdot 10^8$
$\Gamma_{44}$	$1.3787 \cdot 10^6$	$2.3125 \cdot 10^5$	$2.5400 \cdot 10^5$	$7.2969 \cdot 10^5$
$\Gamma_{55}$	$6.7467 \cdot 10^5$	$2.0813 \cdot 10^6$	$1.7140 \cdot 10^6$	$1.0469 \cdot 10^5$
$\Gamma_{66}$	$5.7766 \cdot 10^4$	$2.1724 \cdot 10^4$	$2.9900 \cdot 10^5$	$3.0352 \cdot 10^4$

**Table 2.** The nonzero components of the (6×6) rigidity matrix for the sections H1, H2, H3 and C1.

**6B2. Sectional modes.** For the sections H1, H2, H3, C1 and C2, Figure 11 presents the Poisson’s effects (associated to the axial force and the bending moments) and the out of plane warpings (associated to the shear forces and the torsional moment). However, these sectional modes are given by Figure 12 for the laminated sections C3s and C3a; note that for these sections, each one of the six internal forces contribute to a Poisson’s effect and an out-of plane warping. Besides, some additional sectional distortions are considered for the walled sections H3 and C2 and presented in Figure 13.

**6C. Beam problems: 1D/3D results.** Each beam problem has been computed using the numerical tool CBeam to get the 1D/3D RBT/SV solution and the correspondent 1D/3D SV solution. The 3D results are compared with a full 3D-FEM computation using Abaqus.

Sect.	C2	C3s	C3a
$\Gamma_{11}$	$1.0070 \cdot 10^8$	$2.5017 \cdot 10^6$	$3.7185 \cdot 10^6$
$\Gamma_{22}$	$1.0252 \cdot 10^8$	$7.1272 \cdot 10^5$	$8.2449 \cdot 10^5$
$\Gamma_{33}$	$9.8980 \cdot 10^8$	$1.6309 \cdot 10^7$	$1.6515 \cdot 10^7$
$\Gamma_{44}$	$1.4007 \cdot 10^6$	134.1989	139.7267
$\Gamma_{55}$	$5.1182 \cdot 10^6$	946.9796	$1.1268 \cdot 10^3$
$\Gamma_{66}$	$3.9179 \cdot 10^4$	40.2305	40.0723
$\Gamma_{13}$	$9.4318 \cdot 10^6$	$3.0162 \cdot 10^6$	$-7.1338 \cdot 10^3$
$\Gamma_{14}$			
$\Gamma_{16}$			
$\Gamma_{25}$			
$\Gamma_{36}$			
$\Gamma_{46}$			
		-20.3360	$8.4477 \cdot 10^3$

**Table 3.** The nonzero components of the (6×6) rigidity matrix for the sections C2 and C3.

$r$	1	10	50	100	200
$k_y$	0.8330	0.2087	0.0469	0.0238	0.0120

**Table 4.** The shear coefficient  $k_y$  with respect to the ratios  $r = E_s/E_c$  for the sandwich section C1.

Starting with the same  $[x, y]$ -discretization for the section (used in CSection), the beam is obtained in Abaqus by extrusion (with respect to the beam axis) and the  $z$ -discretization along the span is chosen in line with the  $[x, y]$ -discretization (i.e., in terms of size elements). As finite element, the computations are achieved with the C3D15 nodes quadratic triangular prism.

The comparison between RBT/SV, SV and 3D-FEM results are systematically done for the most important components of the stresses: the axial stresses  $\sigma_{zz}$  and the shear  $\tau = \sqrt{\tau_{xz}^2 + \tau_{yz}^2}$ , at the midspan ( $z = L/2$ ) of the beam and very close to the built-in section ( $0 < z < h/20$ ) simply denoted by  $z_0$  which should read  $z/L \approx 0$ .

**6D. P1: Bending-torsion of a cantilever thick-walled beam.** Figure 14 presents the sectional stress fields for  $\sigma_{zz}$  and  $\tau$  at the midspan and very close to the built-in section. One can note that RBT/SV and 3D-FEM results are in agreement and coincide with those of SV at midspan. Besides, Figure 15 shows the  $z$ -variation of the axial stress  $\sigma_{zz}$  along the span for two point A and B belonging to the extremities of the upper flange of the section. Note that, as expected SV results are the same for both points (for which the axial stresses are due only to the bending), but RBT/SV and 3D-FEM results, which are quite comparable in the major interior area of the beam, show how much the restrained warping (due to the torsion) affects the axial stresses. One can deduce from Figure 15 that the built-in effect spreads over a distance of about  $d \approx 5h = L/2$ .

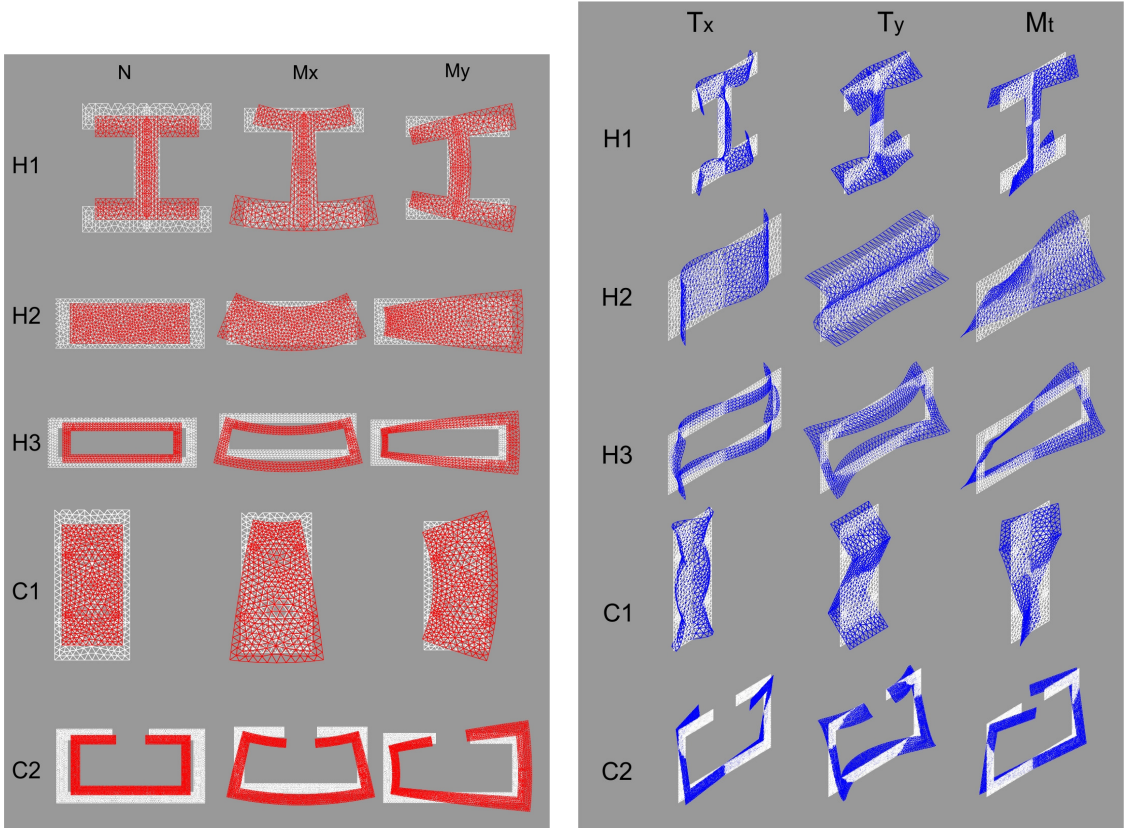


**Figure 11.** Sectional deformations: Poisson's effects and out-of plane warpings.

**6E. P2: Torsion of a cantilever orthotropic beam.** It is known that the restrained warping effect is important for a walled open section subjected to torsion. However this effect can also be important for a compact section when the ratio  $E/G$  is large [El Fatmi and Ghazouani 2011b]. This ratio is about 2.5 for an isotropic material and its value for the present (Mat33) material is about 33. In Figure 16 the stresses provided by RBT/SV and 3D-FEM results are in agreement (in the major part of the beam). Moreover, Figure 17 depicts the  $z$ -variations of the axial stress  $\sigma_{zz}$  for a point A close to a section corner, and the  $z$ -variation of the shear  $\tau$  for the point<sup>14</sup> B in the middle of the big side of the section. Note that, moving from the free end, the shear  $\tau$  vanishes in favor of the axial stress  $\sigma_{zz}$ . RBT/SV and 3D-FEM results are really comparable and show that the built-in effect (related to the restrained torsional warping) spreads over a distance  $d \approx L$  for this compact section; in this case SV's solution is no longer valid to represent the *central* solution.

**6F. P3: Bending of a thin orthotropic box beam.** Figure 18 depicts the 3D deformed shapes obtained by RBT/SV and the 3D-FEM computations. Note the (local) bending of the upper face of the beam due to the loading. To achieve this result, which reflects the location of the load, 8 distortional modes (see

<sup>14</sup>This point B is chosen because it is the point where the shear is maximum for SV's torsion.

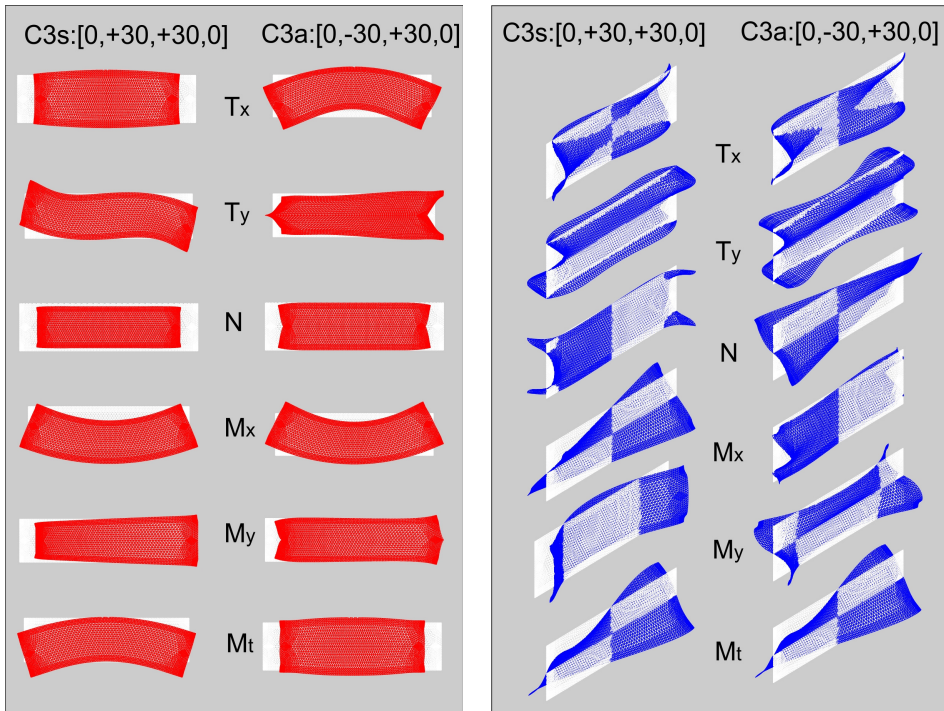


**Figure 12.** Sectional deformations: Poisson’s effects and warpings for the laminated sections.

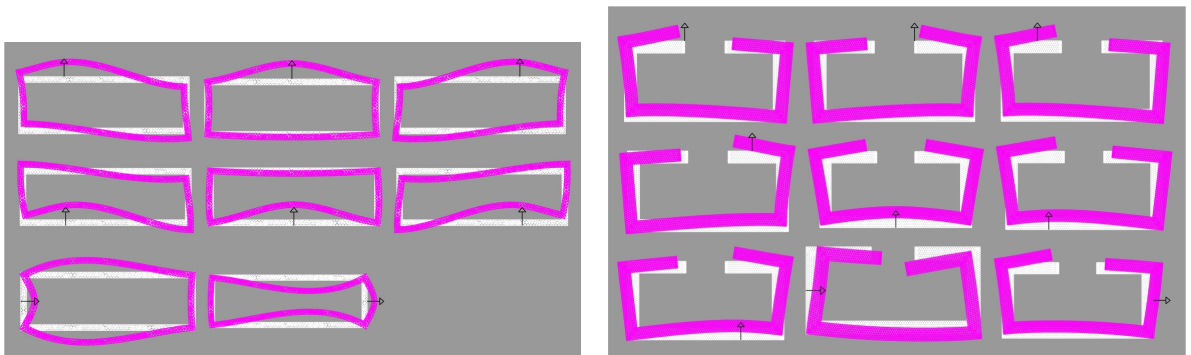


**Figure 13.** Sectional deformations: distortions for the walled sections H3 and C2.

the left side of [Figure 13](#)) have been added to the sectional Poisson’s effects and out-of plane warping modes to be used in RBT/SV.

[Figure 19](#) shows that RBT/SV and 3D-FEM results are mainly in agreement for the axial stress  $\sigma_{zz}$  and the shear  $\tau$  in the midspan and close to the built-in section. Instead of the shear, which is nil in the midspan, the bottom of the right side of [Figure 19](#) compares, the  $\sigma_{xx}$ -field due to the local bending of the upper face of the beam: the results are qualitatively comparable but the magnitude of RBT/SV results are about 50% less than 3D-FEM ones. Thus, using some distortional modes, RBT/SV seems able to

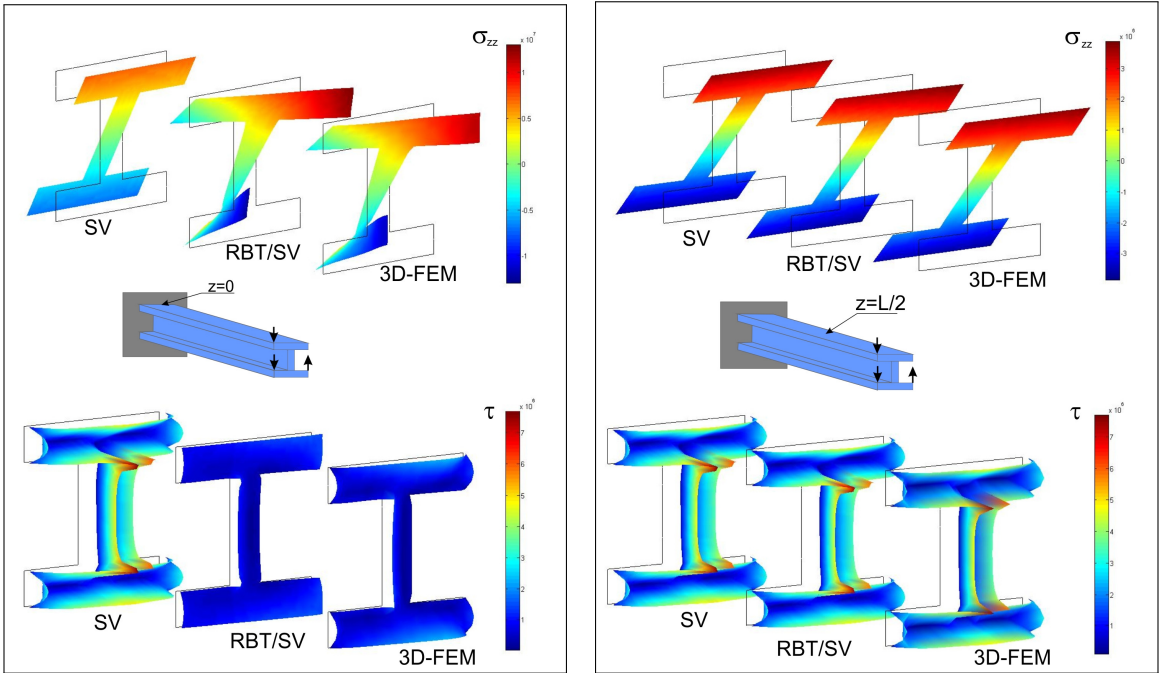


**Figure 14.**  $\sigma_{zz}$  and  $\tau$  fields at  $z=0$  and midspan. Comparison of SV, RBT/SV and 3D-FEM results.

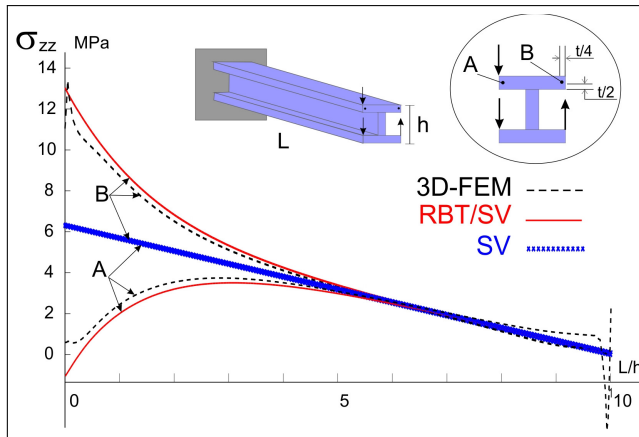


**Figure 15.**  $\sigma_{zz}$ -variations along the span for two points A and B belonging to the upper flange. Comparison of SV, RBT/SV and 3D-FEM results.

account for the location of the loading, which leads in this case to the bending of the upper face of the beam, but the  $\sigma_{xx}$  stress level is underestimated.

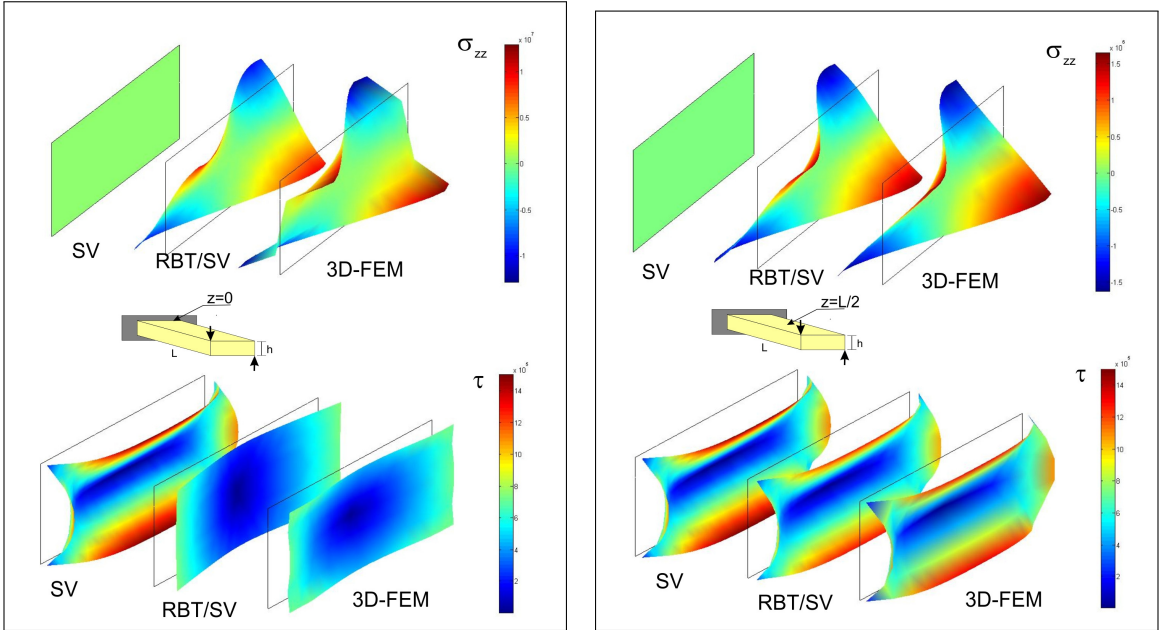


**Figure 16.**  $\sigma_{zz}$  and  $\tau$  fields at  $z=0$  and midspan. Comparison of SV, RBT/SV and 3D-FEM results.

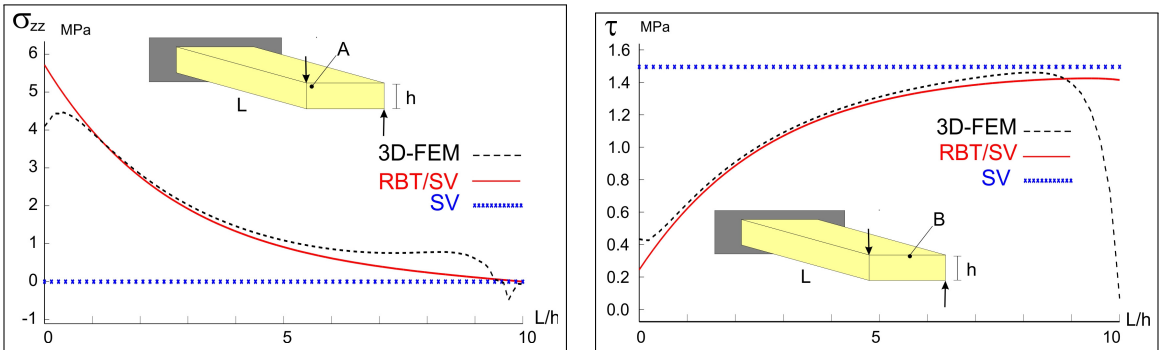


**Figure 17.**  $\sigma_{zz}$ - and  $\tau$ -variation along the span for the points A and B. Comparison of SV, RBT/SV and 3D-FEM results.

**6G. P4: Bending of a sandwich beam strongly contrasted.** The 1D deflection due to the present  $x$ -bending is given by  $u_y(z)$ . Figure 20 compares SV, RBT/SV and 3D-FEM results.<sup>15</sup> The shear force effect is here important and taken into account by TPSV. However, for TPSV, the out-of plane warpings due to the shear force are free at the ends which leads to a more flexible beam behavior. In fact these warpings are restrained right the built-in sections and the deflection appears notably less pronounced as depicted by RBT/SV and 3D-FEM results. It is clear for this example, that these end effects are

<sup>15</sup>For the 3D-FEM results, right to a cross-section at a  $z$  abscissa,  $u_y(z)$  is taken as the average of the 3D displacement with respect to  $y$  axis.

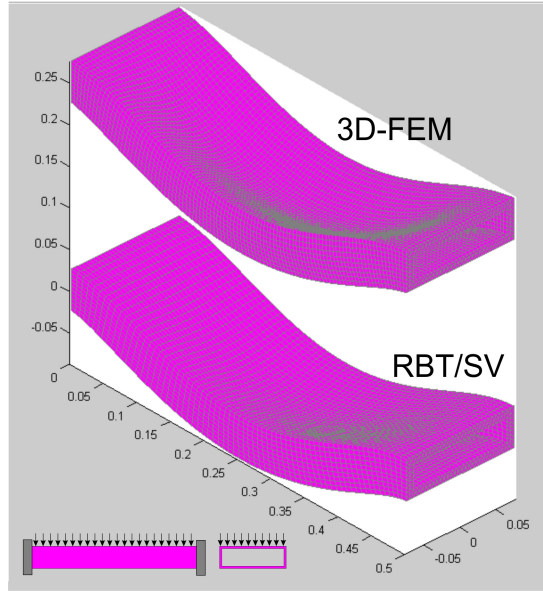


**Figure 18.** 3D deformed shape of the box beam.

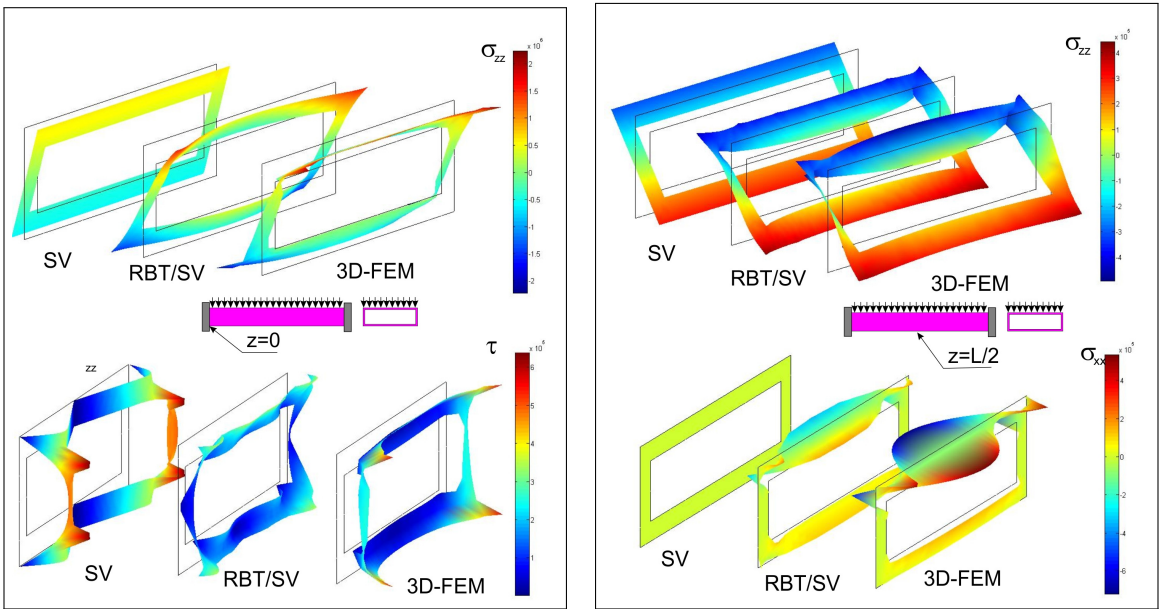


**Figure 19.**  $\sigma_{zz}$ ,  $\tau$  and  $\sigma_{xx}$  fields at  $z=0$  and midspan. Comparison of SV, RBT/SV and 3D-FEM results.

important and dominate the structural behavior of this (strongly contrasted) sandwich beam. For the stresses, Figure 21 shows that RBT/SV and 3D-FEM results are in agreement for the axial stress  $\sigma_{zz}$ , but this is not so true for the shear  $\tau$  even if it is qualitatively acceptable.

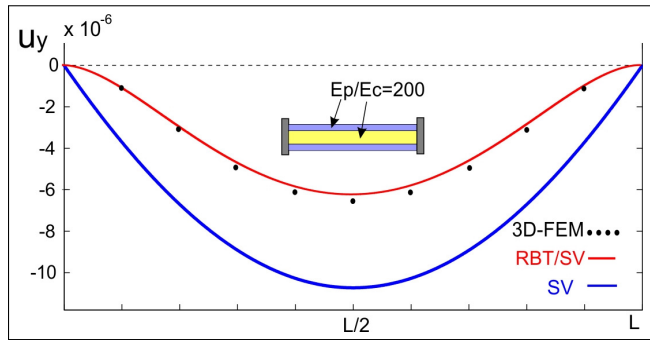


**Figure 20.** Deflection  $u_y$  along the span: SV, RBT/SV and 3D-FEM results.

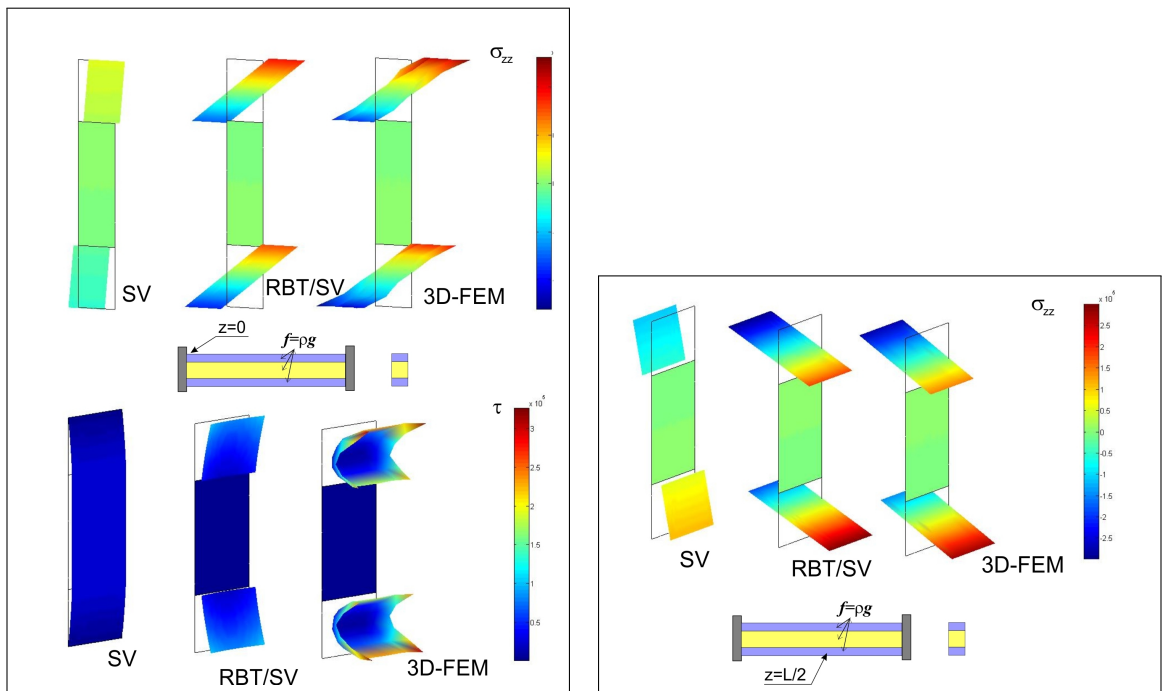


**Figure 21.**  $\sigma_{zz}$  and  $\tau$  fields at  $z_0$  and midspan. Comparison of SV, RBT/SV and 3D-FEM results.

**6H. P5: Bending and torsion of a short unsymmetric open-walled sandwich profile.** For this unsymmetrical section, it is expected that the lateral loading leads to the bending and torsion of the beam as it is shown by the 3D deformed shape given by RBT/SV and 3D-FEM results in Figure 22: note, at the free end, that the out-of plane warping of the section and its shape are relatively well described by RBT/SV result. To obtain this result nine distortional modes (see the right side of Figure 13 have been computed by CSection to be used in RBT/SV. Figure 23 shows that RBT/SV and 3D-FEM results are also in agreement for the axial stress  $\sigma_{zz}$  and the shear  $\tau$  in the midspan and close to the built-in section even if the beam slenderness is here relatively small ( $L/h = 7$ ). For more details, Figure 24 depicts the

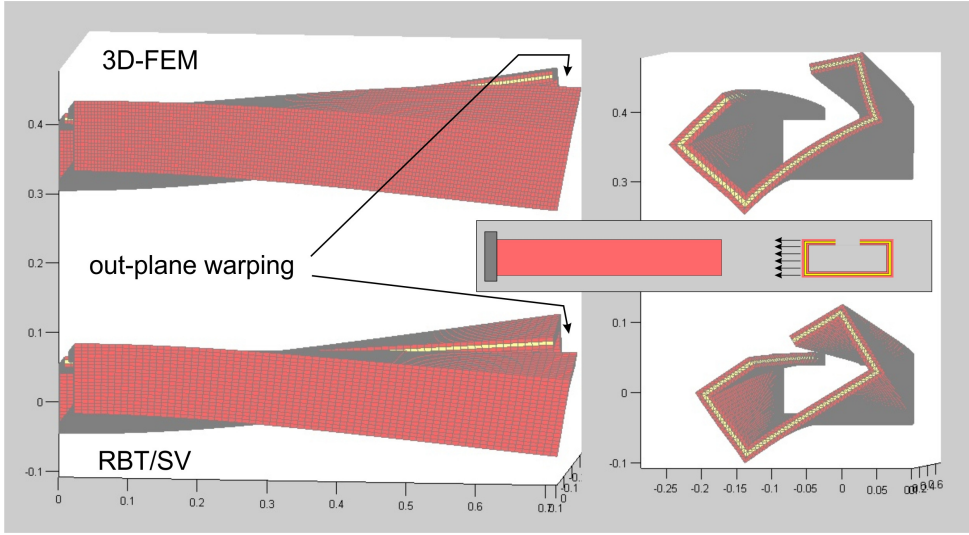


**Figure 22.** 3D deformed shape for the sandwich profile: RBT/SV and 3D-FEM results.

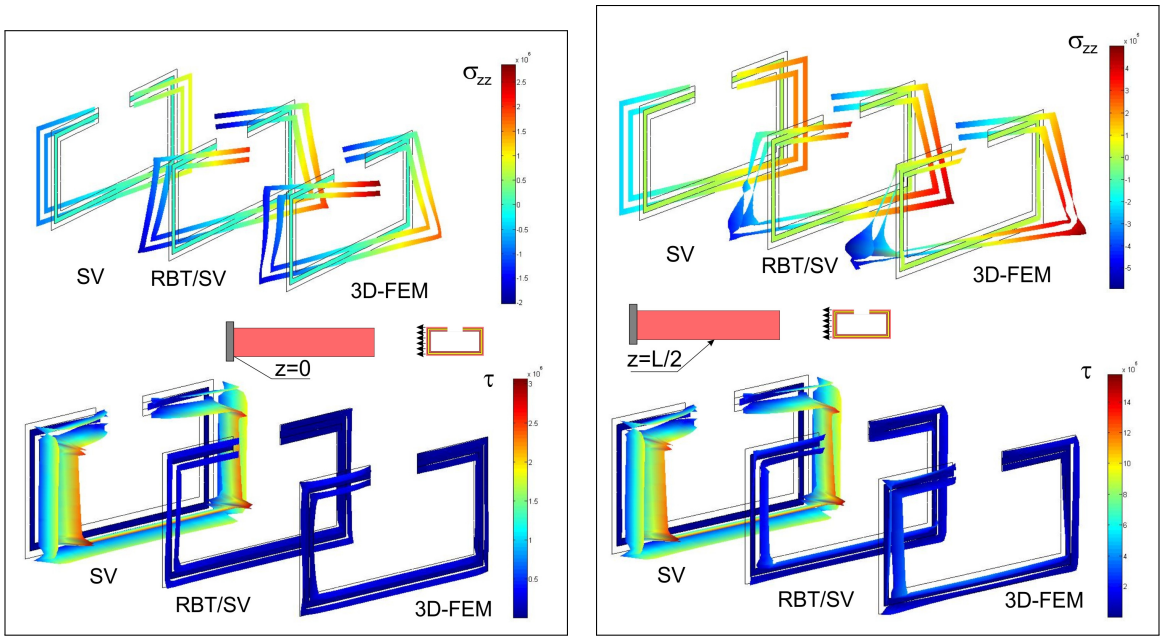


**Figure 23.**  $\sigma_{zz}$  and  $\tau$  fields at  $z=0$  and midspan. Comparison of SV, RBT/SV and 3D-FEM results.

$\sigma_{zz}$ -variations along the span for two points A and B belonging to the skin and the core, respectively; RBT/SV and 3D-FEM results are relatively in agreement and clearly different from that of SV. This is due to the built-in effect (or the restrained warping) which spreads over a distance comparable to the beam length, and dominates the structural beam behavior.

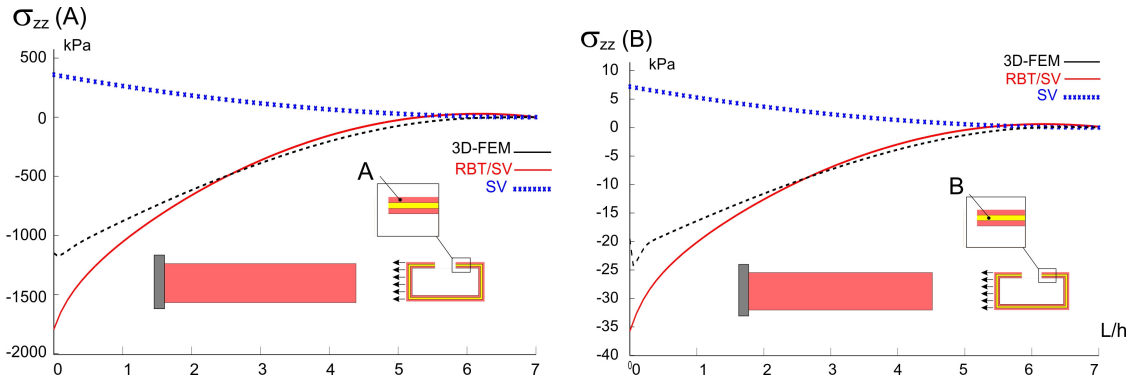


**Figure 24.**  $\sigma_{zz}$ -variations along the span for two points A and B belonging to the skin and the core, respectively. RBT/SV and 3D-FEM results.

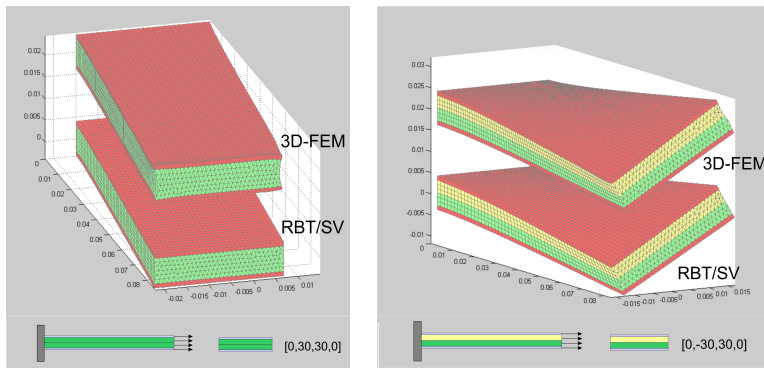


**Figure 25.** 3D deformed shape for the symmetric and antisymmetric laminated beam: RBT/SV and 3D-FEM results.

**6I. P6: Tension of a symmetric/antisymmetric laminated beam.** As expected for these laminate beams the tension leads to a lateral  $y$ -bending for the symmetric case and a torsion for the antisymmetric one, as it is shown by the 3D deformed shapes obtained by both RBT/SV and 3D-FEM computations. In terms of stresses, Figures 26 and 27 show that RBT/SV results are in agreement with the 3D-FEM ones, for both cases, symmetric and unsymmetric. For these cases, the end effects are not important and remain confined close to the ends and SV results appear valid to describe the solution in the major interior area of the beam; thus SV's solution (and hence TPSV) may be used to solve these beam problems, at least for this loading.

### 7. Conclusion

The present refined (1D) beam theory (RBT/SV) is free from all the classical beam assumptions and valid for an arbitrary cross-section. For a composite section, it is worth noting that no homogenization step is needed, and RBT/SV is able to predict the 3D local stresses (the six components of the stress tensor) in each material, which is fundamental for a composite beam.

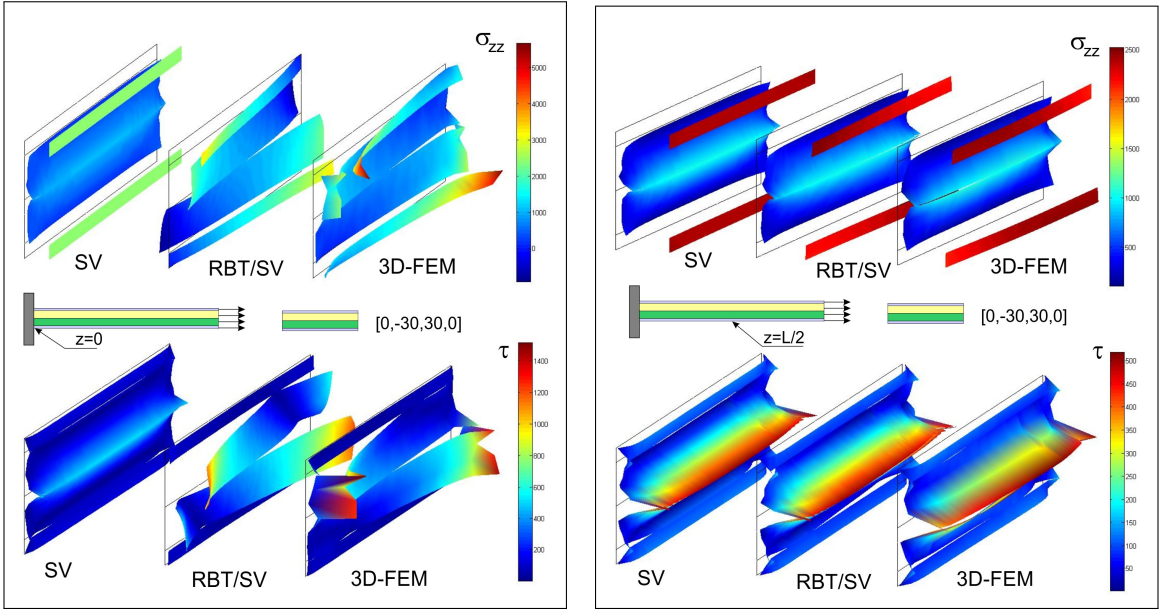


**Figure 26.**  $\sigma_{zz}$  and  $\tau$  fields at  $z_0$  and midspan. Comparison of SV, RBT/SV and 3D-FEM results.

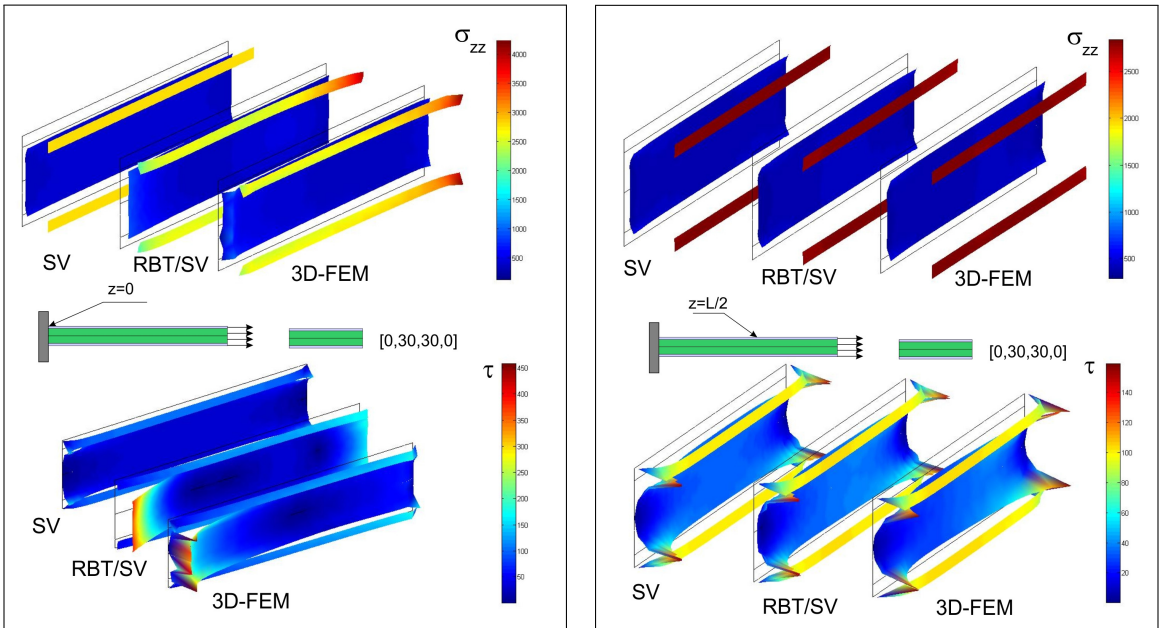


**Figure 27.**  $\sigma_{zz}$  and  $\tau$  fields at  $z_0$  and midspan. Comparison of SV, RBT/SV and 3D-FEM results.

The enrichment of the displacement model uses the main deformation modes of the section (Poisson's effects, out-of plane warpings and distortions). For a given section, these sectional modes being extracted from the correspondent 3D SV's solution, they lead to a beam theory that really fits the section nature (shape and materials).

From the significant set of cross-sections and beam problems presented in this paper, it is clear that RBT/SV is able to describe not only the elastic structural behavior of the beam but also the 3D solution in terms of displacements and stresses in the major interior area of the beam, even if the slenderness is relatively small. Different kinds of 3D effects have been described; these are related to the shape of the section (thin/thick, walled/compact, symmetric/unsymmetric), to its composite nature (anisotropies of the materials, even strongly contrasted) and to the edge effects,<sup>16</sup> especially those due to a built-in section. Theoretically, any boundary condition may be treated, but for the particular case of cantilever or clamped beam, the edge effects appear to be very well described; for other cases, the results on edge effect description will depend on the boundary condition prescribed.

The present refined beam theory may be considered as a *general (1D) beam theory* not only because valid for an arbitrary cross-section (shape and material(s)) but also because it could also be seen as a refinement of SV's approach and hence the correspondent TPSV. Indeed, far from the ends, 3D-RBT/SV results (as 3D-FEM ones) tend toward those of 3D SV's solution when the beam length is sufficiently large (or the ends effects sufficiently small or confined). This result is here expected because RBT/SV is built on SV results: the enrichment in RBT/SV displacement model  $\xi_{\text{RBT/SV}}$ , using the sectional modes extracted from 3D SV's solution, contains the shape of 3D SV displacement  $\xi_{\text{sv}}$  (Equation (8)).

From a practical standpoint, the application of RBT/SV, which deals with detailed results for arbitrary cross-sections, has to be obviously (or inevitably) performed through a numerical way. For that purpose, a package (CSB) of two complementary numerical tools has been developed to accompany RBT/SV: CSection & CBeam. CSection computes by 2D-FEM the sectional characteristics of the cross-section and CBeam uses these characteristics to solve by 1D-FEM the beam problem according to RBT/SV (regardless of the number of the sectional modes available for the cross-section). Thanks to these two steps which combine 2D and 1D computations for the beam, it is possible to recover an important part of the 3D beam behavior, exhibiting detailed 3D effects in terms of displacements and stresses. These numerical tools, which are easy to use, can really help section and beam design and prevent (at least as a first step) the use of costly 3D-FEM computations, especially when working with strongly anisotropic materials and/or thin-walled open/closed profiles. The present work is currently limited to a constant cross-section along the beam axis; its extension to the case of a variable cross-section is under study and will be proposed in a very near future.

## References

- [Alpdogan et al. 2010] C. Alpdogan, S. B. Dong, and E. Taciroglu, "A method of analysis for end and transitional effects in anisotropic cylinders", *Int. J. Solids Struct.* **47** (2010), 947–956.
- [Basaglia et al. 2011] C. Basaglia, D. Camotim, and N. Silvestre, "Non-linear GBT formulation for open-section thin-walled members with arbitrary support conditions", *Comput. Struct.* **89** (2011), 1906–1919.

<sup>16</sup>The edge effects of the free ends depend on the way the tip loads are applied; tip loading and other kinds of boundary conditions need more investigation to obtain a better description of the end-effects they generate.

- [Bebiano et al. 2015] R. Bebiano, R. Gonçalves, and D. Camotim, “A cross-section analysis procedure to rationalise and automate the performance of GBT-based structural analyses”, *Thin-Walled Struct.* **92** (2015), 29–47.
- [Benscoter 1954] S. Benscoter, “A theory of torsion bending for multicell beams”, *J. Appl. Mech. (ASME)* **21**:1 (1954), 25–34.
- [Berdichevsky 1979] V. L. Berdichevsky, “Variational-asymptotic method of constructing a theory of shells”, *Prikl. Mat. Mekh.* **43**:4 (1979), 664–687. In Russian; translated in *J. Appl. Math. Mech.* **43**:4 (1979), 711–736.
- [Blasques 2012] J. P. Blasques, *User’s manual for BECAS: a cross section analysis tool for anisotropic and inhomogeneous beam sections of arbitrary geometry*, v2.0, Technical University of Denmark, Roskilde, Feb. 23, 2012, Available at [http://orbit.dtu.dk/files/7711204/ris\\_r\\_1785.pdf](http://orbit.dtu.dk/files/7711204/ris_r_1785.pdf).
- [Camotim et al. 2006] D. Camotim, N. Silvestre, R. Gonçalves, and P. B. Dinis, “GBT-based structural analysis of thin-walled members: overview, recent progress and future developments”, pp. 187–204 in *Advances in engineering structures, mechanics & construction: proceedings of an international conference on advances in engineering structures, mechanics & construction* (Waterloo, ON, 2006), edited by M. Pandey et al., *Solid Mechanics and Its Applications* **140**, Springer, Dordrecht, 2006.
- [Camotim et al. 2007] D. Camotim, N. Silvestre, and R. Bebiano, “GBT-based local and global vibration analysis of thin-walled members”, pp. 36–76 in *Analysis and design of plated structures, I: Dynamics*, edited by N. E. Shanmugam and C. M. Wang, Woodhead, Cambridge, 2007.
- [Carrera and Giunta 2010] E. Carrera and G. Giunta, “Refined beam theories based on a unified formulation”, *Int. J. Appl. Mech.* **2**:1 (2010), 117–143.
- [Carrera et al. 2011] E. Carrera, G. Giunta, and M. Petrolo, *Beam structures: classical and advanced theories*, Wiley, Chichester, 2011.
- [Carrera et al. 2015] E. Carrera, A. Pagani, M. Petrolo, and E. Zappino, “Recent developments on refined theories for beams with applications”, *Mech. Eng. Rev.* **2**:2 (2015), Article ID #14–00298.
- [Chandra and Chopra 1991] R. Chandra and I. Chopra, “Experimental and theoretical analysis of composite I-beams with-elastic couplings”, *AIAA J.* **29**:12 (1991), 2197–2206.
- [Chandra et al. 1990] R. Chandra, A. D. Stemple, and I. Chopra, “Thin-walled composite beams under bending, torsional and extensional loads”, *J. Aircraft* **27**:7 (1990), 619–626.
- [Dong et al. 2001] S. B. Dong, K. J., and H. Lin, “On Saint-Venant’s problem for an inhomogeneous, anisotropic cylinder, I: Methodology for Saint-Venant solutions”, *J. Appl. Mech. (ASME)* **68**:3 (2001), 376–381.
- [El Fatmi 2007a] R. El Fatmi, “Non-uniform warping including the effects of torsion and shear forces, I: A general beam theory”, *Int. J. Solids Struct.* **44** (2007), 5912–5929.
- [El Fatmi 2007b] R. El Fatmi, “Non-uniform warping including the effects of torsion and shear forces, II: Analytical and numerical applications”, *Int. J. Solids Struct.* **44** (2007), 5930–5952.
- [El Fatmi 2007c] R. El Fatmi, “Non-uniform warping theory for beams”, *C. R. Mécanique* **335** (2007), 467–474.
- [El Fatmi 2012] R. El Fatmi, “A Matlab tool to compute the mechanical characteristics of any composite section”, *Rev. Compos. Matér. Av.* **22**:3 (2012), 395–413.
- [El Fatmi and Ghazouani 2011a] R. El Fatmi and N. Ghazouani, “A higher order composite beam theory built on 3D Saint Venant’ solution, part-I: Theoretical developments”, *Compos. Struct.* **93** (2011), 557–566.
- [El Fatmi and Ghazouani 2011b] R. El Fatmi and N. Ghazouani, “A higher order composite beam theory built on 3D Saint Venant’ solution, part-2: Built-in effect influence on the behavior of end-loaded cantilever beams”, *Compos. Struct.* **93** (2011), 567–581.
- [El Fatmi and Zenzri 2002] R. El Fatmi and H. Zenzri, “On the structural behavior and the Saint Venant solution in the exact beam theory: application to laminated composite beams”, *Comput. Struct.* **80**:16-17 (2002), 1441–1456.
- [El Fatmi and Zenzri 2004] R. El Fatmi and H. Zenzri, “A numerical method for the exact elastic beam theory: Applications to homogeneous and composite beams”, *Int. J. Solids Struct.* **41**:9–10 (2004), 2521–2537.
- [Ferrero et al. 2001] J. F. Ferrero, J. J. Barrau, J. M. Segura, B. Castanie, and M. Sudre, “Torsion of thin-walled composite beams with midplane symmetry”, *Compos. Struct.* **54** (2001), 111–120.
- [Genoese et al. 2014a] A. Genoese, A. Genoese, A. Bilotta, and G. Garcea, “A composite beam model including variable warping effects derived from a generalized Saint Venant solution”, *Compos. Struct.* **110** (2014), 140–151.

- [Genoese et al. 2014b] A. Genoese, A. Genoese, A. Bilotta, and G. Garcea, “A generalized model for heterogeneous and anisotropic beams including section distortions”, *Thin-Walled Struct.* **74** (2014), 85–103.
- [Giavotto et al. 1983] V. Giavotto, M. Borri, P. Mantegazza, G. Ghiringhelli, V. Carmaschi, G. C. Maffioli, and F. Mussi, “Anisotropic beam theory and applications”, *Comput. Struct.* **16** (1983), 403–413.
- [Horgan and Simmonds 1991] C. O. Horgan and J. G. Simmonds, “Asymptotic analysis of an end-loaded, transversely isotropic, elastic, semi-infinite strip weak in shear”, *Int. J. Solids Struct.* **27**:15 (1991), 1895–1914.
- [Horgan and Simmonds 1994] C. O. Horgan and J. G. Simmonds, “Saint Venant end effects in composite structures”, *Compos. Eng.* **4**:3 (1994), 279–286.
- [Iesan 1976] D. Iesan, “Saint-Venant’s problem for inhomogeneous and anisotropic elastic bodies”, *J. Elasticity* **6** (1976), 277–294.
- [Jung et al. 2007] S. N. Jung, I.-J. Park, and E. S. Shin, “Theory of thin-walled composite beams with single and double cell sections”, *Compos. B Eng.* **38** (2007), 182–192.
- [Kim and White 1997] C. Kim and R. S. White, “Thick-walled composite beam theory including 3D elastic effects and torsional warping”, *Int. J. Solids Struct.* **34**:31-32 (1997), 4237–4259.
- [Kim et al. 2006] N.-I. Kim, D. K. Shin, and M.-Y. Kim, “Exact solutions for thin-walled open-section composite beams with arbitrary lamination subjected to torsional moment”, *Thin-Walled Struct.* **44** (2006), 638–654.
- [Ladevèze and Simmonds 1998] P. Ladevèze and J. G. Simmonds, “New concepts for linear beam theory with arbitrary geometry and loading”, *Eur. J. Mech. A Solids* **17**:3 (1998), 377–402.
- [Lee and Lee 2004] J. Lee and S.-h. Lee, “Flexural-torsional behavior of thin-walled composite beams”, *Thin-Walled Struct.* **42** (2004), 1293–1305.
- [Loughlan and Ata 1998] J. Loughlan and M. Ata, “The analysis of carbon fibre composite box beams subjected to torsion with variable twist”, *Comput. Methods Appl. Mech. Eng.* **152** (1998), 373–391.
- [Pluzsik and Kollar 2006] A. Pluzsik and L. Kollar, “Torsion of closed section, orthotropic, thin-walled beams”, *Int. J. Solids Struct.* **43** (2006), 5307–5336.
- [Polit et al. 2015] O. Polit, L. Gallimard, P. Vidal, M. D’Ottavio, G. Giunta, and S. Belouettar, “An analysis of composite beams by means of hierarchical finite elements and a variables separation method”, *Comput. Struct.* **158** (2015), 15–29.
- [Rand 1998] O. Rand, “Interlaminar shear stresses in solid composite beams using a complete out of plane shear deformation model”, *Comput. Struct.* **66**:6 (1998), 713–723.
- [Rand 2000] O. Rand, “On the importance of cross-sectional warping in solid composite beams”, *Compos. Struct.* **49** (2000), 393–397.
- [Rappel and Rand 2000] O. Rappel and O. Rand, “Analysis of elastically coupled thick-walled composite blades”, *Int. J. Solids Struct.* **37** (2000), 1019–1043.
- [Roberts and Al-Ubaidi 2001] T. M. Roberts and H. Al-Ubaidi, “Influence of shear deformation on restrained torsional warping of pultruded FRP bars of open cross-section”, *Thin-Walled Struct.* **39** (2001), 395–414.
- [Sapountzakis and Mokos 2007] E. J. Sapountzakis and V. G. Mokos, “3D beam element of composite cross section including warping and shear deformation effects”, *Comput. Struct.* **85** (2007), 102–116.
- [Schardt 1994] R. Schardt, “Generalized beam theory: An adequate method for coupled stability problems”, *Thin-Walled Struct.* **19** (1994), 161–180.
- [Silvestre et al. 2011] N. Silvestre, D. Camotim, and N. F. Silva, “Generalized beam theory revisited: From the kinematical assumptions to the deformation mode determination”, *Int. J. Struct. Stab. Dyn.* **11**:5 (2011), 969–997.
- [Toupin 1965] R. A. Toupin, “Saint-Venant’s principle”, *Arch. Ration. Mech. Anal.* **18** (1965), 83–96.
- [Vlasov 1959] V. Z. Vlasov, Тонкостенные упругие стержни, Fizmatgiz, Moscow, 1959. Translated as *Thin-walled elastic beams*, 2nd ed., National Technical Information Service, Jerusalem, 1961.
- [Volovoi et al. 1999] V. V. Volovoi, D. H. Hodges, V. L. Berdichevsky, and V. G. Sutyryn, “Asymptotic theory for static behavior of elastic anisotropic I-beams”, *Int. J. Solids Struct.* **36**:7 (1999), 1017–1043.
- [Volovoi et al. 2001] V. V. Volovoi, D. H. Hodges, C. E. S. Cesnik, and B. Popescu, “Assessment of beam modeling methods for rotor blade applications”, *Math. Comput. Model.* **33** (2001), 1099–1112.

[Yu et al. 2005] W. Yu, D. H. Hodges, V. V. Volovoi, and E. D. Fuchs, “A generalized Vlasov theory for composite beams”, *Thin-Walled Struct.* **43** (2005), 1493–1511.

[Yu et al. 2012] W. Yu, D. H. Hodges, and J. C. Ho, “Variational asymptotic beam sectional analysis—an updated version”, *Int. J. Eng. Sci.* **59** (2012), 40–64.

Received 31 Aug 2015. Revised 28 Dec 2015. Accepted 5 Jan 2016.

RACHED EL FATMI: [rached.elfatmi@enit.rnu.tn](mailto:rached.elfatmi@enit.rnu.tn)

*Ecole Nationale d'Ingénieurs de Tunis, Université de Tunis El Manar, LGC, BP 37, Le Belvédère, 1002 Tunis, Tunisia*

# JOURNAL OF MECHANICS OF MATERIALS AND STRUCTURES

[msp.org/jomms](http://msp.org/jomms)

Founded by Charles R. Steele and Marie-Louise Steele

## EDITORIAL BOARD

ADAIR R. AGUIAR	University of São Paulo at São Carlos, Brazil
KATIA BERTOLDI	Harvard University, USA
DAVIDE BIGONI	University of Trento, Italy
YIBIN FU	Keele University, UK
IWONA JASIUK	University of Illinois at Urbana-Champaign, USA
C. W. LIM	City University of Hong Kong
THOMAS J. PENCE	Michigan State University, USA
GIANNI ROYER-CARFAGNI	Università degli studi di Parma, Italy
DAVID STEIGMANN	University of California at Berkeley, USA
PAUL STEINMANN	Friedrich-Alexander-Universität Erlangen-Nürnberg, Germany

## ADVISORY BOARD

J. P. CARTER	University of Sydney, Australia
D. H. HODGES	Georgia Institute of Technology, USA
J. HUTCHINSON	Harvard University, USA
D. PAMPLONA	Universidade Católica do Rio de Janeiro, Brazil
M. B. RUBIN	Technion, Haifa, Israel

**PRODUCTION** [production@msp.org](mailto:production@msp.org)

SILVIO LEVY Scientific Editor

---

Cover photo: Mando Gomez, [www.mandolux.com](http://www.mandolux.com)

See [msp.org/jomms](http://msp.org/jomms) for submission guidelines.

---

JoMMS (ISSN 1559-3959) at Mathematical Sciences Publishers, 798 Evans Hall #6840, c/o University of California, Berkeley, CA 94720-3840, is published in 10 issues a year. The subscription price for 2016 is US \$575/year for the electronic version, and \$735/year (+\$60, if shipping outside the US) for print and electronic. Subscriptions, requests for back issues, and changes of address should be sent to MSP.

---

JoMMS peer-review and production is managed by EditFLOW<sup>®</sup> from Mathematical Sciences Publishers.

PUBLISHED BY

 **mathematical sciences publishers**  
nonprofit scientific publishing

<http://msp.org/>

© 2016 Mathematical Sciences Publishers

<b>What discrete model corresponds exactly to a gradient elasticity equation?</b>	<b>VASILY E. TARASOV</b>	<b>329</b>
<b>A refined 1D beam theory built on 3D Saint-Venant's solution to compute homogeneous and composite beams</b>	<b>RACHED EL FATMI</b>	<b>345</b>
<b>A unified theory for constitutive modeling of composites</b>	<b>WENBIN YU</b>	<b>379</b>
<b>Modeling and experimentation of a viscoelastic microvibration damper based on a chain network model</b>	<b>CHAO XU, ZHAO-DONG XU, TENG GE and YA-XIN LIAO</b>	<b>413</b>
<b>An anisotropic piezoelectric half-plane containing an elliptical hole or crack subjected to uniform in-plane electromechanical loading</b>	<b>MING DAI, PETER SCHIAVONE and CUN-FA GAO</b>	<b>433</b>
<b>On the causality of the Rayleigh wave</b>	<b>BARIŞ ERBAŞ and ONUR ŞAHİN</b>	<b>449</b>
<b>On the modeling of dissipative mechanisms in a ductile softening bar</b>	<b>JACINTO ULLOA, PATRICIO RODRÍGUEZ and ESTEBAN SAMANIEGO</b>	<b>463</b>